AMERICAN MUSEUM NOVITATES

Number 4003, 36 pp. November 9, 2023

Glacial Relicts? A New Scorpion from Mount Olympus, Greece (Euscorpiidae: *Euscorpius*)

JAVIER BLASCO-ARÓSTEGUI[1] AND LORENZO PRENDINI[2]

ABSTRACT

Mediterranean mountains and Pleistocene glacial cycles are responsible for much of the unique biodiversity of the Western Palearctic, acting respectively as refugia and drivers of diversification. Mount Olympus, a legendary Greek landmark, is a perfect example. This massif provided a glacial refugium for many species, resulting in a unique biota. In the present contribution, a new euscorpiid scorpion with a distinctive morphology, *Euscorpius olympus*, sp. nov., is described from an isolated population in the foothills of Mount Olympus. This new species raises the number of species in the genus *Euscorpius* Thorell, 1876, to 74, in Greece to 32, and in the vicinity of Mount Olympus, to three. The roles of climatic oscillations, altitudinal gradients and habitat heterogeneity on the diversity and distributions of the three species occurring around Mount Olympus are briefly discussed.

INTRODUCTION

Mediterranean mountains are among the primary hotspots of biodiversity in the Western Palearctic (Hewitt, 1996; Cuttelod et al., 2009; Klesser et al., 2021). These mountain ranges shaped diversity and distributions across the region by serving as refugia during Quaternary glaciations

[1] Centre for Ecology, Evolution and Environmental Changes, Departamento de Biologia Animal, Faculdade de Ciências, Universidade de Lisboa, Lisbon; and Arachnology Lab and Scorpion Systematics Research Group, Division of Invertebrate Zoology, American Museum of Natural History.

[2] Arachnology Lab and Scorpion Systematics Research Group, Division of Invertebrate Zoology, American Museum of Natural History.

 ISSN 0003-0082

(Coope, 1994; Médail and Diadema, 2009; Platania et al., 2020; Costa et al., 2023), sheltering populations that either recolonized other areas during more favorable interglacial stages or remained isolated throughout the Last Glacial Maximum (Hewitt, 1999, 2004; Ursenbacher et al., 2006; Schmitt, 2007; Drovetski et al., 2018). Altitudinal and latitudinal shifts affected by orogenic processes and climatic oscillations also provided opportunities for adaptation (Hewitt, 2000, 2004; Minachilis et al., 2020). Consequently, much of the biodiversity and endemism around the Mediterranean Basin is attributed to diversification associated with the glacial-interglacial period (Cuttelod et al., 2009; Médail and Diadema, 2009; Blondel et al., 2010; Costa et al., 2023).

The Iberian, Italian and Balkan peninsulas represent some of the most important glacial refugia in the southern part of the Western Palearctic (Hewitt, 1999; Ursenbacher et al., 2006; Schmitt, 2007; Baselga, 2008; Costa et al., 2023). The mountain ranges of these peninsulas often shelter endemic taxa (Baselga, 2008; Blondel et al., 2010). One such example is Mount Olympus, a legendary Greek landmark well known for its unique biodiversity. The mountain and its vicinity served as a glacial refugium during the Pleistocene Ice Age (Hewitt, 2004; Schmitt, 2007; Médail and Diadema, 2009). Severe climatic oscillations, together with altitudinal gradients and the availability of microrefugia (e.g., caves and relictual forests), shaped its biodiversity (Strid, 1980; Stamou et al., 1984; Mauries, 2003; Minachilis et al., 2020, 2023). Around 1700 species of plants, 40 mammals, 100 birds, 34 amphibians and reptiles, and 300 invertebrates, including at least three species of scorpions in two families (Fet et al., 2018), inhabit the massif, 56 species of which (26 plants and 30 invertebrates) are endemic.

The family Euscorpiidae Laurie, 1896, exhibits a disjunct distribution in the Neotropics (Mexico and Guatemala) and the Palearctic (Europe and northern Africa). It is the most speciose scorpion family in Europe, currently comprising three genera and 94 species (Parmakelis et al., 2013; Fet et al., 2016; Štundlová et al., 2019; Podnar et al., 2021, 2022; Tropea et al., 2022; Kovařík et al., 2023) distributed across a variety of humid to semihumid habitats from the islands and coastlines of the Mediterranean to the high altitudes of the Alps and other mountain ranges (fig. 1A). Despite being the most well-studied European scorpion family, the taxonomy of Euscorpiidae remains problematic for several reasons, including the morphological similarity of many species, which requires adult males for accurate diagnosis and delimitation; an inadequate understanding of species distributions that has, in recent years, revealed several cases of sympatry; a general failure to identify adequate diagnostic morphological characters and present comparative diagnoses; the absence of workable taxonomic keys; and different interpretations of species limits, caused in part by the inconsistent application of alternative sources of evidence including morphology, short fragments of mitochondrial DNA, and karyotype (Fet and Soleglad, 2002; Parmakelis et al., 2013; Štundlová et al., 2019; Podnar et al., 2021).

Seventy-three (78%) of the Palearctic species of Euscorpiidae belong to the genus *Euscorpius* Thorell, 1876, 31 (42%) of which occur in Greece, including two species from the vicinity of Mount Olympus (figs. 1B, 2), *Euscorpius kinzelbachi* Tropea et al., 2014, and an undetermined species in the *Euscorpius sicanus* (C.L. Koch, 1837) complex (Tropea et al., 2014; Fet et al., 2018), referred to hereafter as *Euscorpius* aff. *sicanus*. In the present contribution, a new scorpion with a distinctive morphology, *Euscorpius olympus*, sp. nov., is described from a distinct microhabitat in the foothills

of Mount Olympus (figs. 1–4). This new species raises the number of species in the genus *Euscorpius* to 74, in Greece to 32 (table 1), and in the vicinity of Mount Olympus, to three. The roles of climatic oscillations, altitudinal gradients and habitat heterogeneity on the diversity and distributions of the three species occurring around Mount Olympus are briefly discussed.

MATERIAL AND METHODS

Specimens were hand collected from deep crevices in limestone rocks, using forceps, a pickaxe and portable ultraviolet (UV) light emitting diode (LED) flashlights (Stahnke, 1972). Material, preserved in 70% ethanol for morphological examination and 95% ethanol for DNA isolation, is deposited in the collections of the American Museum of Natural History (AMNH), New York, and the Ambrose Monell Cryocollection for Molecular and Microbial Research (AMCC) at the AMNH.

Morphological terminology follows Prendini et al. (2003) for carapace topography and surface ornamentation; Loria and Prendini (2014) for lateral ocelli; Vachon (1952) and Prendini (2000) for carinae and surfaces of pedipalps and legs, replacing "external" and "internal" with "retrolateral" and "prolateral" respectively; Prendini (2000) for the patellar process, a spiniform apophysis on the prolateral surface of the pedipalp patella, teleologically referred to as the "patellar spur" in some literature; Vachon (1963) for cheliceral dentition, replacing "external" and "internal" with "retrolateral" and "prolateral" respectively; Prendini and Loria (2020) for lobes and notches on pedipalp chela fingers; Vachon (1952, 1981) for trichobothrial notation, with trichobothrial homology following Stockwell (1989), in part; a modified version of Prendini (2004) for tergal, sternal, and metasomal carinae; Stockwell (1989) and Ochoa et al. (2010) for general description of hemispermatophore; Kovařík et al. (2020), adapted from Vachon (1948), for terminology of the hemispermatophore capsular region; Vachon (1952) and Stahnke (1970) for other characters.

Live habitus photographs were taken in the field with a Nikon D3500 camera, using a Sigma 105 mm macro lens. Digital images of preserved specimens were taken in visible and long-wave UV light using a Microptics™ ML-1000 digital photomicrography system at the AMNH. Morphological examination of specimens was conducted using a Nikon SMZ1500 stereoscope. Measurements (tables 2, 3) were taken following Stahnke (1970) and Sissom et al. (1990), using the ocular micrometre of a Nikon SMZ1500 stereoscope.

The type locality of the field-collected material was georeferenced using a portable Garmin 64s GPS Navigation System. Two-dimensional and three-dimensional distribution maps were created using QGIS v.3.4 (Quantum QGIS Development Team, 2023) by superimposing georeferenced point localities on a digital elevation layer from DIVA-GIS (https://www.diva-gis.org/data). The three-dimensional map was produced using the QGIS plug-in 'Qgis2threejs' on the elevation layer to create a Digital Elevation Model representing Mount Olympus and plotting the species locality records along its altitudinal gradient. Precise records of *Euscorpius* in the surroundings of Mount Olympus were extracted from the material examined and published literature, e.g., Tropea et al. (2014).

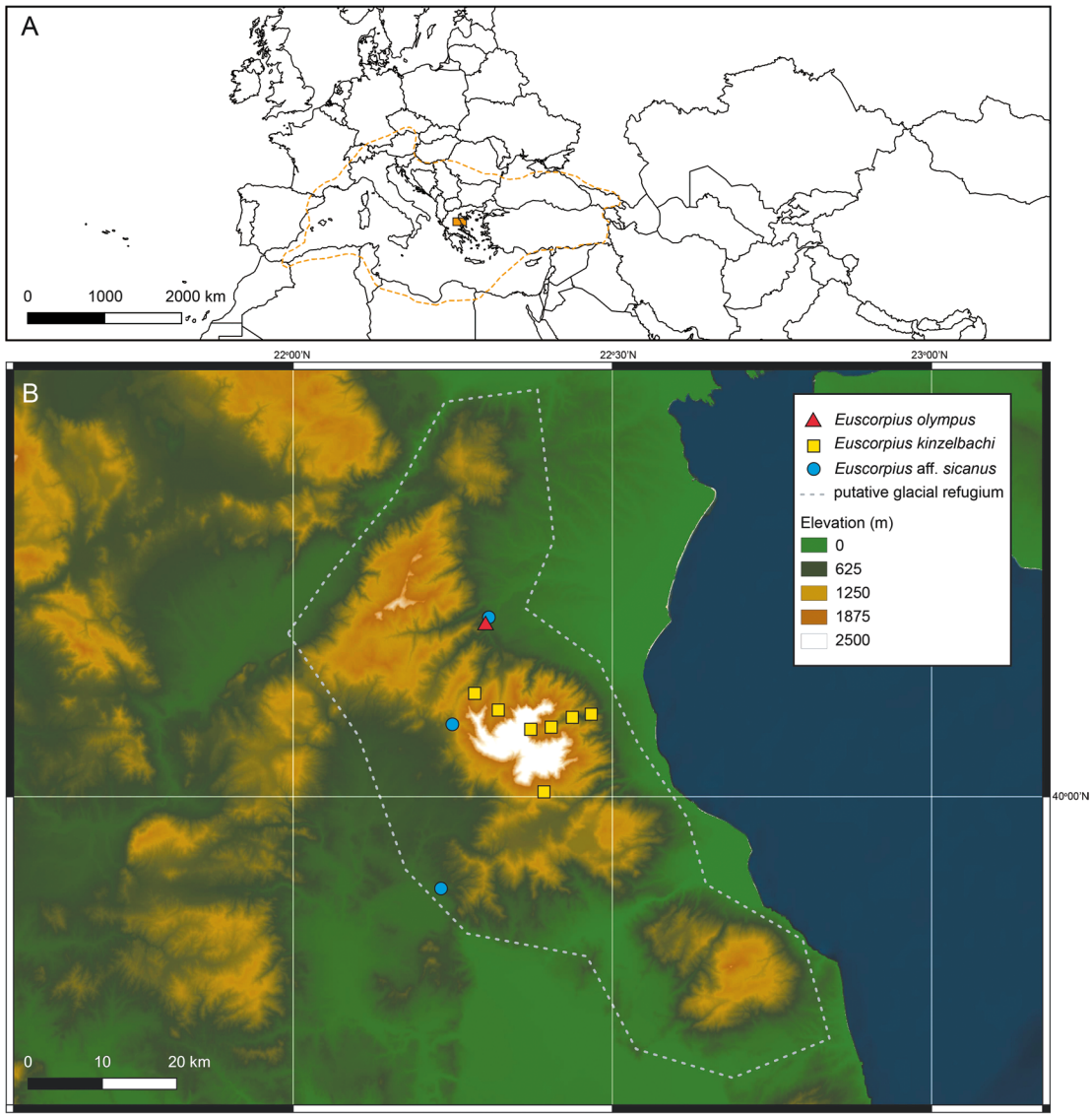

FIGURE 1. **A.** Map of the Western Palearctic with international borders. Shaded orange rectangle indicates area in **B**. Dashed orange line indicates boundary of outermost records of *Euscorpius* Thorell, 1876. **B.** Map of eastern Greece. Dashed grey line illustrates putative glacial refugia (Médail and Diadema, 2009). Colored symbols represent locality records of *Euscorpius olympus*, sp. nov. (red triangle), *Euscorpius kinzelbachi* Tropea et al., 2014 (yellow squares), and *Euscorpius* aff. *sicanus* (blue circles).

COMPARATIVE MATERIAL EXAMINED

Euscorpius aquilejensis (C.L. Koch, 1837): **ITALY: Friuli-Venezia Giulia:** *Udine Prov.*: Aquileia, along Via Antica, 45°46′15.2″N 13°22′16.1″E, 52 m, 9.xiii.2021, J. Blasco-Aróstegui and A. Calatayud-Mascarell, rock and mud walls, 4 ♂, 1 ♀ (AMNH), 6 ♀ (AMCC [LP 17180, 17189, 17190, 17193, 17295, 17328]). **Trentino-Alto Adigio:** *Trento Prov.*: Ala, 45°45′09.7″N

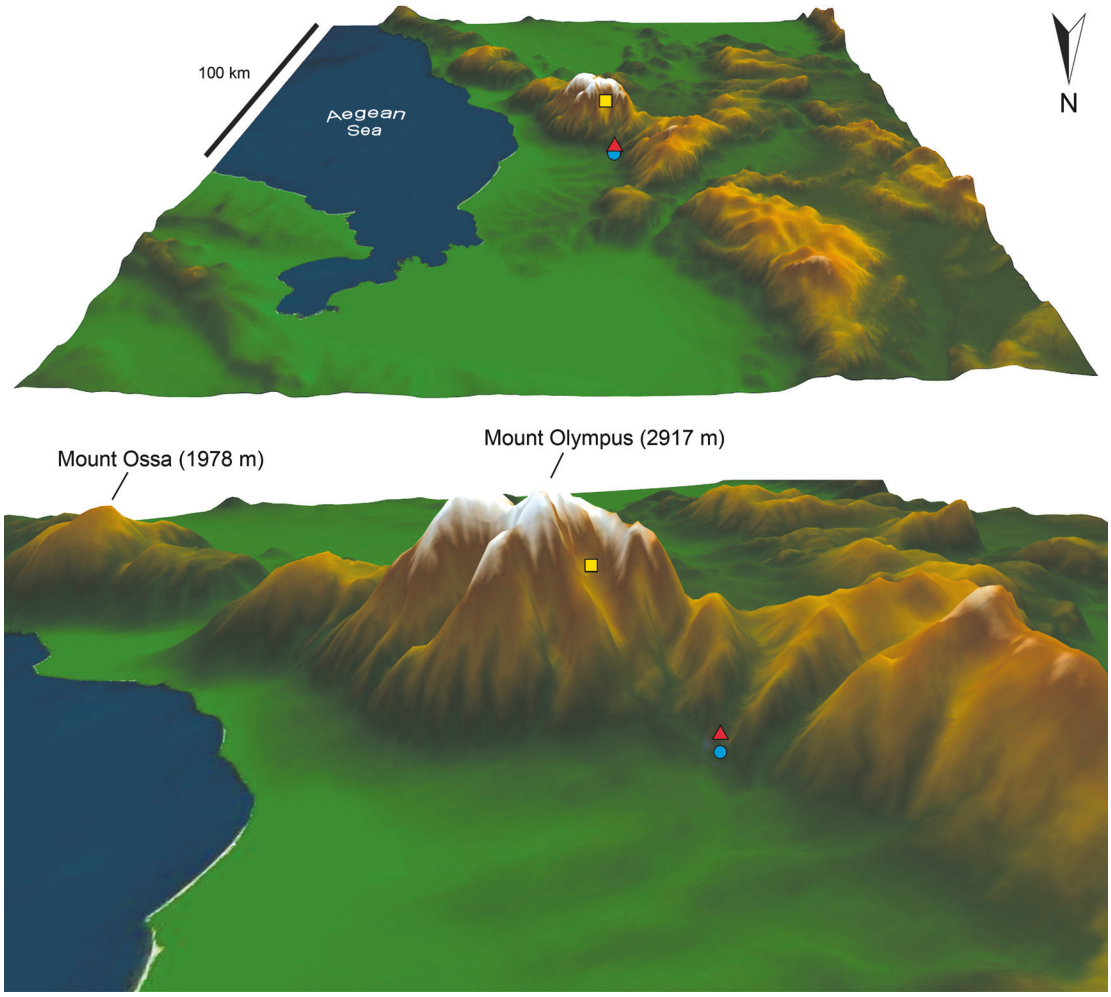

FIGURE 2. Three-dimensional representation of Mount Olympus and vicinity, including Mount Ossa and coastline of Aegean Sea. Colored symbols represent locality records of *Euscorpius olympus*, sp. nov. (red triangle), *Euscorpius kinzelbachi* Tropea et al., 2014 (yellow square), and *Euscorpius* aff. *sicanus* (blue circle).

10°59′55.6″E, 215 m, 4.xiii.2021, J. Blasco-Aróstegui and A. Calatayud-Mascarell, rock walls of park in middle of town and walls surrounding vineyard on outskirts, 2 ♂, 4 ♀ (AMNH); Roveretto, 45°51′17.5″N 11°01′00.7″E, 223 m, 4.xiii.2021, J. Blasco-Aróstegui and A. Calatayud-Mascarell, woods around town, 4 ♂ (AMNH), 2 ♀ (AMCC [LP 17181, 17252]).

Euscorpius kinzelbachi Tropea et al., 2014: **GREECE: Central Macedonia Region:** *Pieria Regional Unit*: Mount Olympus National Park, Mount Olympus, near Spilios Agapitos Refuge, 40°04′48″N 22°22′23″E, 2038 m, 21.v.2018, S. Schaffrath and M. Porschen, in dead tree, 1 ♀ (AMNH), 2 ♀ (AMCC [LP 16164, 16165]); Mount Olympus, Naoum Cave, 40°06′11.8″N 22°19′18.3″E, 1361 m, 24.vi.2023, J. Blasco-Aróstegui, 6 ♂, 4 ♀ (AMNH); Mount Olympus, Tsoureka Spring, 40°07′24.7″N 22°17′08.1″E, 1162 m, 24.vi.2023, J. Blasco-Aróstegui, 5 ♂, 2 ♀, (AMNH).

FIGURE 3. *Euscorpius olympus*, sp. nov., live habitus, dorsal aspect. **A.** Holotype ♂ (AMNH). **B.** Paratype ♀ (AMNH).

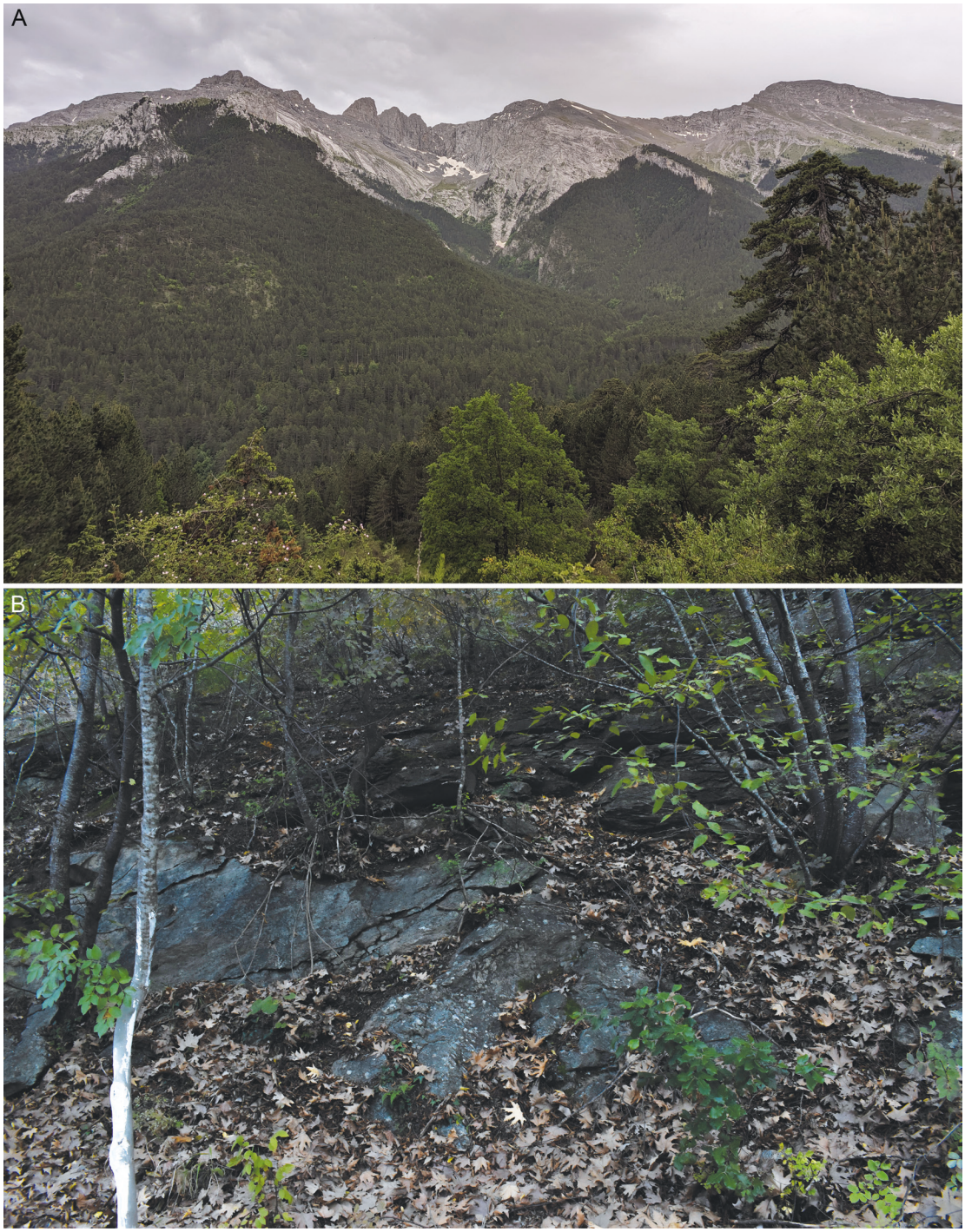

FIGURE 4. *Euscorpius olympus*, sp. nov., habitat at type locality. **A.** Peaks and mixed forests on slopes of Mount Olympus, Greece. **B.** Microhabitat, crevices in limestone rocks in predominantly deciduous forest in northern foothills of Mount Olympus.

TABLE 1. Species of *Euscorpius* Thorell, 1876, recorded from Greece, indicating major areas of occurrence. Asterisks denote 25 species endemic to the country.

Euscorpius amorgensis Tropea et al., 2017*	Cyclades Islands: Amorgos
Euscorpius avcii Tropea et al., 2012	North Aegean Islands: Samos
Euscorpius birulai Fet et al., 2014*	Central Greece: Euboea Island
Euscorpius candiota Birula, 1903*	Cyclades Islands: Crete
Euscorpius corcyraeus Tropea and Rossi, 2012*	Ionian Islands: Corfu
Euscorpius curcici Tropea et al., 2017*	Cyclades Islands: Sikinos
Euscorpius drenskii Tropea et al., 2015	Central Macedonia: Chalkidiki Peninsula
Euscorpius erymanthius Tropea et al., 2013*	Western Greece: Mount Erymanthos
Euscorpius giachinoi Tropea and Fet, 2015*	Western and Central Greece
Euscorpius italicus (Herbst, 1800)	Epirus
Euscorpius kabateki Kovařík and Šťáhlavský, 2020*	Central Greece: Mount Parnassos
Euscorpius kinzelbachi Fet et al., 2014*	Central Macedonia: Mount Olympus
Euscorpius koschewnikowi Birula, 1900*	Central Macedonia: Mount Athos
Euscorpius kritscheri Fet et al., 2013*	Cyclades Islands: Tinos
Euscorpius lesbiacus Tropea et al., 2020*	North Aegean Islands: Lesvos
Euscorpius mylonasi Fet et al., 2014*	Central Greece: Euboea Island
Euscorpius naupliensis (C.L. Koch, 1837)*	Western Greece and Peloponnese
Euscorpius olympus, sp. nov.*	Central Macedonia: Mount Olympus
Euscorpius ossae (Caporiacco, 1950)*	Thessaly: Mount Ossa
Euscorpius popovi Tropea et al., 2015	Central Macedonia: Chalkidiki Peninsula
Euscorpius scaber Birula, 1900*	Central Macedonia: Chalkidiki Peninsula
Euscorpius scheraboni Kovařík and Šťáhlavský, 2020*	Attica: Mount Hymettos
Euscorpius aff. *sicanus**	Thessaly: including Mount Olympus
Euscorpius simaiakisi Tropea et al., 2022*	Cyclades Islands: Andros
Euscorpius solegladi Fet et al., 2014	Central Macedonia: Chalkidiki Peninsula
Euscorpius stahlavskyi Tropea et al., 2014*	Epirus: Mount Smolikas
Euscorpius sulfur Kovařík et al., 2023	Epirus: Sulfur Cave
Euscorpius tauricus (C.L. Koch, 1837)	Cyclades Islands: Naxos and Paros
Euscorpius triantisi Tropea et al., 2022*	Sporades Islands: Skyros
Euscorpius vailatii Tropea and Fet, 2015*	Western and Central Greece
Euscorpius vignai Tropea et al., 2014*	Dodecanese Islands: Karpathos and Kasos
Euscorpius yagmuri Kovařik et al., 2014*	Epirus

Euscorpius aff. *sicanus*: **GREECE: Central Macedonia Region:** *Pieria Regional Unit*: Foteina, 2 km SE on road to Agios Dimitrios, 40°12′28.1″N 22°18′05.3″E, 461 m, 24.v.2018, S. Schaffrath and M. Bläser, cracks in rocky slope with vegetation, 1 ♂, 3 ♀ (AMCC [LP 16173–16176]); Foteina, road exiting village, along foothills of Mount Olympus, 40°12′28.5″N 22°18′05.3″E, 509 m, 23.x.2021, J. Blasco-Aróstegui and A. Calatayud-Mascarell, deciduous forest slope, in leaf litter and under rocks, 2 ♂ (AMNH), 3 ♀ (AMCC [LP 17873, 17883, 17962]). Kokkinopilos, mountain slope 1.5 km S, 40°03′51.8″N 22°14′59.5″E, 1030 m, 24.v.2018, S. Schaffrath and M. Bläser, under loose stones with residual moisture on dry sandy slope, 6 ♀ (AMCC [LP 16178–16183]). **Thessaly Region:** *Larissa Regional Unit*: Tsaritsani, 1 km NE, 39°53′22.1″N 22°13′54.6″E, 514 m, 24.v.2018, S. Schaffrath and M. Bläser, dry stony slope, in cracks and under loose stones, 2 ♀ (AMCC [LP 16184, 16185]).

SYSTEMATICS

Family Euscorpiidae Laurie, 1896

Euscorpius Thorell, 1876

***Euscorpius olympus*, sp. nov.**

Figures 1–19; tables 1–4

Type Material: **GREECE: Central Macedonia:** *Pieria Regional Unit*: Holotype ♂ (AMNH), Foteina, road exiting village, along foothills of Mount Olympus, 40°12′28.5″N 22°18′05.3″E, 509 m, 26.x.2021, J. Blasco-Aróstegui and A. Calatayud-Mascarell, deciduous forest slope with several rocks, in deep crevices. Paratypes: 1 subad. ♀ (AMCC [LP 16177]), Foteina, 2 km SE on road to Agios Dimitrios, 40°12′28.1″N 22°18′05.3″E, 461 m, 24.v.2018, S. Schaffrath and M. Bläser, night with UV light, cracks in rocky slope with vegetation; 1 ♀ (AMNH), 3 ♀ (AMCC [LP 17925, 17932, 17940]), 1 juv. ♂ (AMCC [LP 17986]), same data as holotype; 8 ♂, 7 ♀ (AMNH), Foteina, road exiting village, along foothills of Mount Olympus, 40°12′28.5″N 22°18′05.3″E, 509 m, 24. vi.2023, J. Blasco-Aróstegui; 2 ♂, 2 ♀ (AMNH), Foteina, secondary trail originating from main road, 40°12′36.4″N 22°18′07.8″E, 499 m, 24.vi.2023, J. Blasco-Aróstegui.

Diagnosis: *Euscorpius olympus*, sp. nov., most closely resembles *E. aquilejensis*, a widespread species distributed from the southeastern Italian Peninsula to Slovenia and Croatia (Tropea, 2013a). The two species are somewhat similar in coloration, with a slender, elongated pedipalp chela, similar trichobothrial patterns, and a broad telson in both sexes. However, *E. olympus* differs from *E. aquilejensis* in the following respects. *Euscorpius olympus* is a proportionally larger species, measuring 38.2–48.4 mm in length (fig. 5; tables 2, 3), whereas *E. aquilejensis* is medium-sized, usually measuring 29–38 mm but occasionally reaching 41 mm (Tropea, 2013a). The subdistal teeth on the movable finger of the chelicera are clearly separated in *E. olympus*, but almost united, forming a bicuspid in *E. aquilejensis*. The carapace anterior margin possesses a shallow median notch in *E. olympus* (fig. 6) but is sublinear in *E. aquilejensis*. The carapace surface is almost asetose in the male of *E. olympus* (fig. 6), but noticeably more

TABLE 2. Measurements (mm) of *Euscorpius olympus*, sp. nov., male type material, deposited in the American Museum of Natural History (AMNH), New York. Abbreviations: H, height; L, length; W, width. Notes: [1]sum of prosoma, mesosoma, and metasoma; [2]sum of tergites I–VII, measured along midline; [3]sum of metasomal segments I–V and telson; [4]sum of pedipalp femur, patella, and chela; [5]measured from movable finger condyle to fingertip; [6]measured at median notch; [7]measured at median lobe.

		Holotype	Paratypes			
		♂	♂	♂	♂	♂
		AMNH	AMNH	AMNH	AMNH	AMNH
Total length[1]		44.2	48.1	48.4	40.9	45.7
Carapace	L	6.1	6.5	6.7	5.8	6.6
	anterior W	3.5	3.7	4.1	3.3	3.6
	posterior W	5.5	6.0	6.5	5.7	6.2
Median ocelli	ocular W	0.8	0.8	0.8	0.7	0.8
	interoc. distance	0.3	0.3	0.3	0.3	0.4
	ocular diameter	0.2	0.2	0.2	0.2	0.2
Mesosoma	L[2]	11.1	14.7	16.9	14.3	13.5
Metasoma	L[3]	27	26.9	24.8	20.8	25.6
Segment I	L	2.7	2.8	2.6	2.0	2.4
	W	2.0	2.0	1.9	1.8	2.1
	H	1.8	2.2	2.0	1.7	1.9
Segment II	L	3.2	3.3	2.8	2.3	3.0
	W	1.8	1.8	1.8	1.7	1.8
	H	1.5	2.1	1.9	1.6	1.8
Segment III	L	3.3	3.6	3.1	2.6	3.5
	W	1.6	1.7	1.7	1.6	1.7
	H	1.7	2.0	1.9	1.6	1.7
Segment IV	L	4.1	4.0	3.6	3.0	3.8
	W	1.5	1.7	1.7	1.5	1.6
	H	1.6	2.0	1.7	1.5	1.6
Segment V	L	6.6	6.6	5.9	5.2	6.1
	W	1.4	1.6	1.6	1.4	1.6
	H	1.7	2.0	1.8	1.5	1.6
Telson	L	6.6	6.6	6.8	5.7	6.8
Vesicle	L	5.0	5.2	5.3	4.4	5.3
	W	2.9	2.3	2.5	2.1	2.3
	H	3.0	2.7	2.8	2.5	2.7
Aculeus	L	1.6	1.6	1.5	1.3	1.5
Pedipalp	L[4]	25.1	26.8	26.9	22.8	26.4
Femur	L	6.1	6.4	6.6	5.5	6.5
	W	2.0	2.1	2.2	1.7	2.2
	H	1.0	1.2	1.1	1.0	1.1
Patella	L	5.8	6.1	6.4	5.3	6.3
	W	2.2	2.3	2.4	2.0	2.4
	H	1.6	1.7	1.8	1.5	1.6
Chela	L[5]	13.2	14.3	13.9	12.0	13.6
Manus	L	7.5	7.9	8.1	6.8	8.0
	W	4.0	4.2	4.4	3.6	4.3
	H	2.7	3.2	3.3	2.5	3.2
Fixed finger	L	5.8	6.4	5.8	5.2	5.6
	W[6]	0.4	0.5	0.6	0.4	0.5
	H[6]	0.7	0.7	0.8	0.7	0.7
Movable finger	L	7.1	7.0	7.2	6.9	7.2
	W[7]	0.3	0.3	0.4	0.3	0.4
	H[7]	0.9	1.1	1.1	0.8	1.1
Pectines	L	2.9	3.0	3.2	2.8	2.8

TABLE 3. Measurements (mm) of *Euscorpius olympus*, sp. nov., female type material, deposited in the American Museum of Natural History (AMNH), New York, including the Ambrose Monell Cryocollection for Molecular and Microbial Research (AMCC). Abbreviations: H, height; L, length; W, width. Notes: [1]sum of prosoma, mesosoma, and metasoma; [2]sum of tergites I–VII, measured along midline; [3]sum of metasomal segments I–V and telson; [4]sum of pedipalp femur, patella, and chela; [5]measured from movable finger condyle to fingertip; [6]measured at median notch; [7]measured at median lobe.

		Paratypes				
		♀ AMNH	♀ AMNH	♀ AMCC [LP 17925]	♀ AMCC [LP 17932]	♀ AMCC [LP 17940]
Total length[1]		41.3	46.7	45.6	38.2	44.7
Carapace	L	6.7	6.9	6.4	5.6	6.6
	anterior W	3.9	4.1	3.9	3.3	3.9
	posterior W	5.9	6.4	6.2	5.4	6.2
Median ocelli	ocular W	0.7	0.9	0.8	0.7	0.8
	interoc. distance	0.3	0.4	0.3	0.2	0.3
	ocular diameter	0.2	0.2	0.2	0.2	0.2
Mesosoma	L[2]	17.8	14.6	16.4	13.6	16.3
Metasoma	L[3]	16.8	25.2	22.8	19	21.8
Segment I	L	2.2	2.5	2.0	1.9	2.0
	W	1.9	2.3	1.9	1.9	1.9
	H	1.8	1.8	1.6	1.6	1.5
Segment II	L	2.8	3.0	2.3	2.2	2.3
	W	1.7	1.9	1.7	1.8	1.7
	H	1.7	1.7	1.5	1.5	1.4
Segment III	L	3.0	3.3	3.0	2.3	3.1
	W	1.6	1.8	1.6	1.7	1.6
	H	1.6	1.6	1.7	1.5	1.3
Segment IV	L	3.4	4.0	3.7	2.9	3.3
	W	1.5	1.7	1.5	1.6	1.5
	H	1.5	1.5	1.5	1.4	1.3
Segment V	L	5.4	6.5	6.0	4.9	5.5
	W	1.4	1.6	1.4	1.5	1.4
	H	1.6	1.6	1.6	1.5	1.3
Telson	L	5.2	6.1	5.8	4.8	5.6
Vesicle	L	3.6	4.1	4.1	3.5	3.8
	W	1.7	2.1	1.8	1.8	1.7
	H	1.7	2.0	1.7	1.6	1.6
Aculeus	L	1.6	2.0	1.7	1.3	1.8
Pedipalp	L[4]	24.9	26.8	26.3	22	25.3
Femur	L	6.1	6.7	6.7	5.6	6.2
	W	2.1	2.2	2.1	1.7	1.8
	H	1.4	1.4	1.0	1.0	1.0
Patella	L	5.9	6.3	6.0	5.3	6.0
	W	2.3	2.4	2.3	1.8	2.2
	H	1.6	1.8	1.8	1.4	1.5
Chela	L[5]	12.9	13.8	13.6	11.1	13.1
Manus	L	6.9	7.8	7.8	6.7	7.6
	W	3.5	4.2	3.9	3.5	4.0
	H	2.6	2.6	2.4	2.3	2.3
Fixed finger	L	5.4	6.0	5.5	4.6	5.5
	W[6]	0.4	0.6	0.5	0.4	0.5
	H[6]	0.8	1.0	0.9	0.8	0.8
Movable finger	L	6.0	7.4	7.2	5.9	6.9
	W[7]	0.5	0.7	0.6	0.3	0.4
	H[7]	0.9	1.1	1.1	0.9	0.9
Pectines	L	2.3	2.3	2.3	2.2	2.3

setose in the male of *E. aquilejensis*. The carapace lateral surfaces and pedipalp femur prodorsal surface are less finely and sparsely granular in *E. olympus* (figs. 6, 7A, B) than *E. aquilejensis*. The medial lobe of the pedipalp chela movable finger is rounded in the male of *E. olympus* (fig. 8B) but slightly conical in the male of *E. aquilejensis*. The ventromedian row of spinules on the leg IV telotarsi comprise 10–13 short, blunt spinules in *E. olympus* (fig. 10A–D) and 9–11 elongate spinules in *E. aquilejensis*. The median lateral carinae of metasomal segment I are obsolete and incomplete, restricted to the anterior half of the segment in *E. olympus* (figs. 11B, 12B), but distinct and complete in *E. aquilejensis*.

Euscorpius olympus may be separated from the other two species of *Euscorpius* occurring in the vicinity of Mount Olympus as follows. The carapace, tergites and metasomal segments are uniformly dark brown in *E. olympus* (fig. 3) but variably dark brown with light brown infuscation in *E.* aff. *sicanus* and, to a lesser extent, *E. kinzelbachi*. The carapace anterior margin possesses a shallow median notch in *E. olympus* (fig. 6) but is sublinear in *E. kinzelbachi* and *E.* aff. *sicanus*. The carapace surface is entirely finely and sparsely granular, more densely so laterally, in *E. olympus* (fig. 6) but smooth, except for the lateral surfaces which are finely and sparsely granular, in *E. kinzelbachi*. The pedipalp femur is more elongated (width 32% of length) in *E. olympus* than in *E. kinzelbachi* (width 37.4% of length) and *E.* aff. *sicanus* (width 38.3% of length; tables 2, 3). The retrodorsal carina of the femur is obsolete, comprising small granules in *E. olympus* (figs. 7A, B, 16A) but distinct, comprising large granules in *E. kinzelbachi* and *E.* aff. *sicanus*. The patellar process is more developed in *E. olympus* (height : width 137.5%) than *E.* aff. *sicanus* (height : width, 102.9%). Although the trichobothria of the patellar retrolateral surface are similar in all three species, each comprising six trichobothria in the *et* series (fig. 16C), *E.* aff. *sicanus* often possesses an additional *et* trichobothrium, whereas *E. kinzelbachi* sometimes lacks an *et* trichobothrium, possessing only five trichobothria in the series. Additionally, both *E. olympus* and *E. kinzelbachi* possess only four trichobothria in the *eb* series (fig. 16C), whereas *E.* aff. *sicanus* possesses five. The pedipalp chela of *E. olympus* is slenderer and elongate in both sexes than the chelae of *E. kinzelbachi* and *E.* aff. *sicanus* which are shorter and broader (fig. 15). The retroventral carina of the chela is costate-granular and more pronounced in *E. olympus* than *E. kinzelbachi* and *E.* aff. *sicanus* (figs. 8, 9, 15). In the male of *E. olympus*, the medial lobe of the chela movable finger fits evenly with the medial notch of the fixed finger, leaving little to no gap between the fingers, when closed, unlike the males of *E. kinzelbachi* and *E.* aff. *sicanus*, in which the medial lobe fits unevenly with the medial notch, creating a distinct gap between the fingers, when closed (fig. 15). Furthermore, the medial lobe and notch are broad and shallow in the female of *E. olympus*, whereas the lobe is distinct and rounded, the notch deep in the female of *E. kinzelbachi*, and the lobe absent or obsolete, the notch distinct in the female of *E.* aff. *sicanus* (fig. 15). The pectinal tooth counts of *E. olympus* are lower, 8/8 (♂) or 7/7 (♀) (fig. 6; table 4), than the counts of *E.* aff. *sicanus*, 10/10 (♂) or 8–9/8–9 (♀). The spinules in the ventromedian row of the leg telotarsi are short and blunt (fig. 10) in *E. olympus* but elongate in *E. kinzelbachi* and *E.* aff. *sicanus*. The telson is relatively slender and shallowly convex ventrally in the male of *E. olympus* (fig. 14A, B), as in the male of *E. kinzelbachi*, but markedly globose in the male of *E.* aff. *sicanus*.

FIGURE 5. *Euscorpius olympus*, sp. nov., habitus, dorsal (**A, C**) and ventral (**B, D**) aspects. **A, B.** Paratype ♂ (AMNH). **C, D.** Paratype ♀ (AMNH). Scale bar = 10 mm

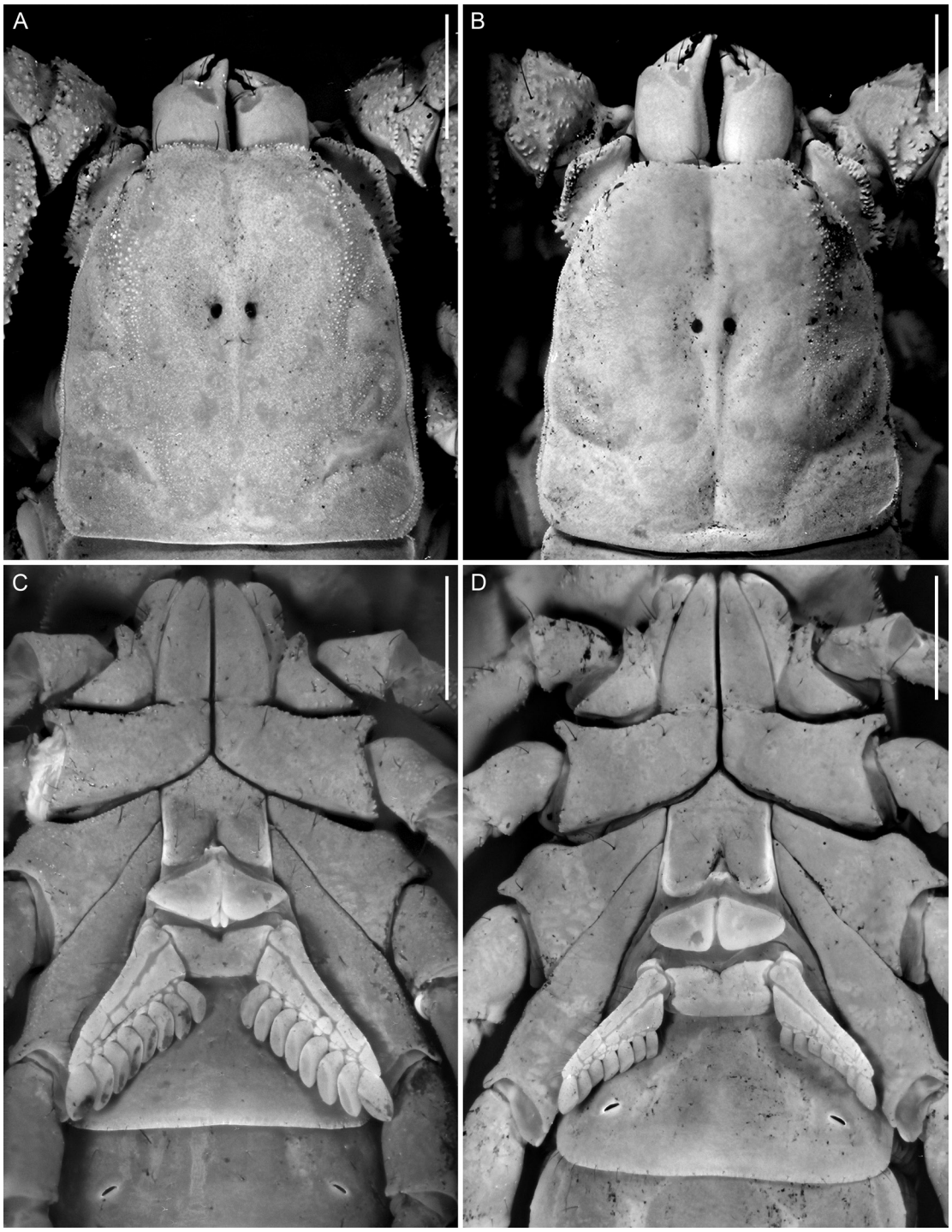

FIGURE 6. *Euscorpius olympus*, sp. nov., carapace, dorsal aspect (**A, B**) and sternum and pectines, ventral aspect (**C, D**). **A, C.** Holotype ♂ (AMNH). **B, D.** Paratype ♀ (AMNH). Scale bars = 2 mm.

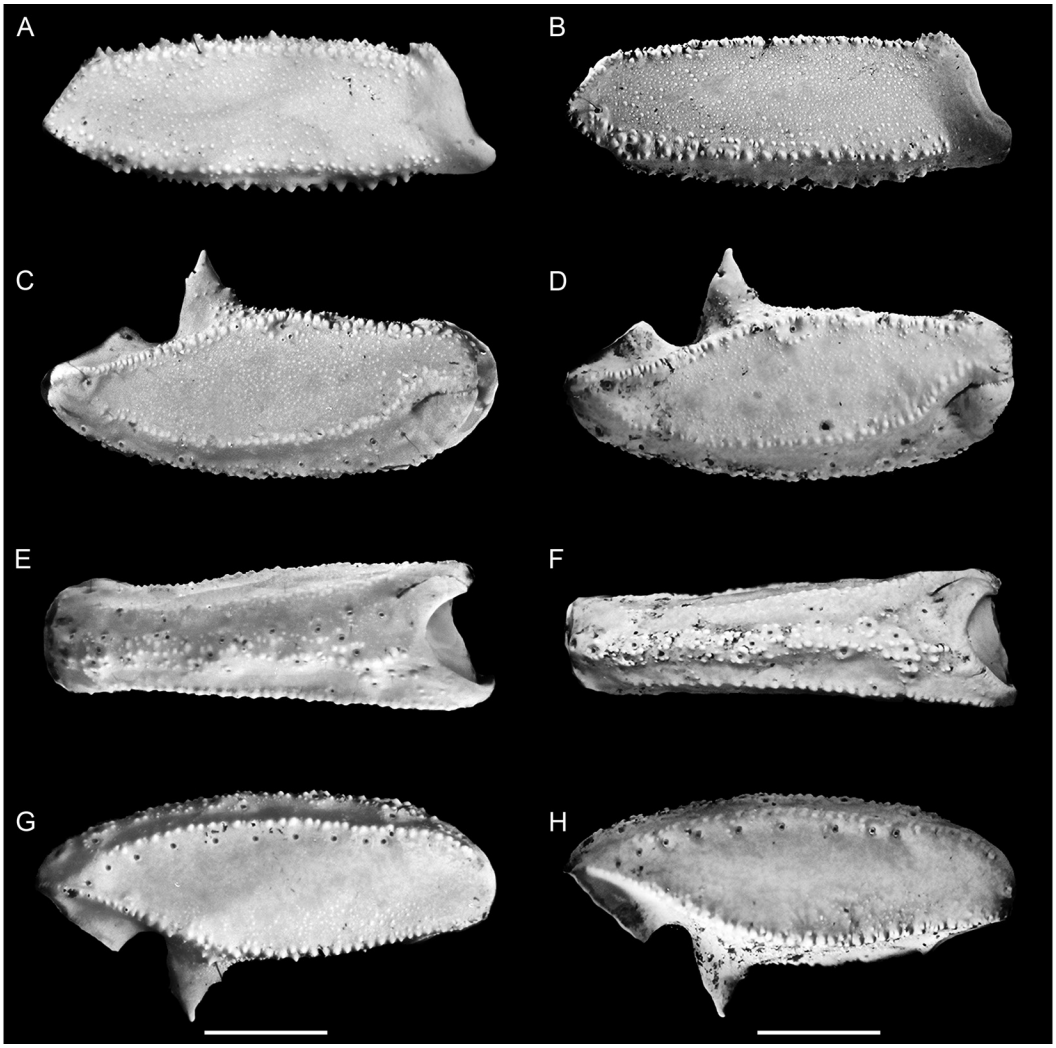

FIGURE 7. *Euscorpius olympus*, sp. nov., dextral pedipalp femur, dorsal aspect (**A, B**), and patella, dorsal (**C, D**), retrolateral (**E, F**) and ventral (**G, H**) aspects. **A, C, E, G.** Holotype ♂ (AMNH). **B, D, F, H.** Paratype ♀ (AMNH). Scale bars = 2 mm.

The hemispermatophore of *E. olympus* differs markedly from that of the other two species (figs. 18, 19). Whereas the flagellar lamina of *E. olympus* is rounded distally and lacks a constriction proximally, the lamina of *E. kinzelbachi* and *E.* aff. *sicanus* tapers distally and exhibits a marked constriction proximally. The capsule of *E. olympus* bears two distinct lateral lobes each terminating in a crownlike structure ("dorsal trough margin" sensu Sissom, 1994: 269–270; "tube-like structure" sensu Soleglad and Sissom, 2001: 56), two distal external lobes, two distal internal lobes and two basal lobes (fig. 18D), whereas the capsule of *E. kinzelbachi* and *E.* aff. *sicanus* exhibits only one of each (fig. 18E, F). The shape of the distal external lobe also differs among the three species, with a more flattened dorsal process and acute proximal termination in *E. olympus* (fig. 19D); a semicircular structure terminating in an abrupt invagina-

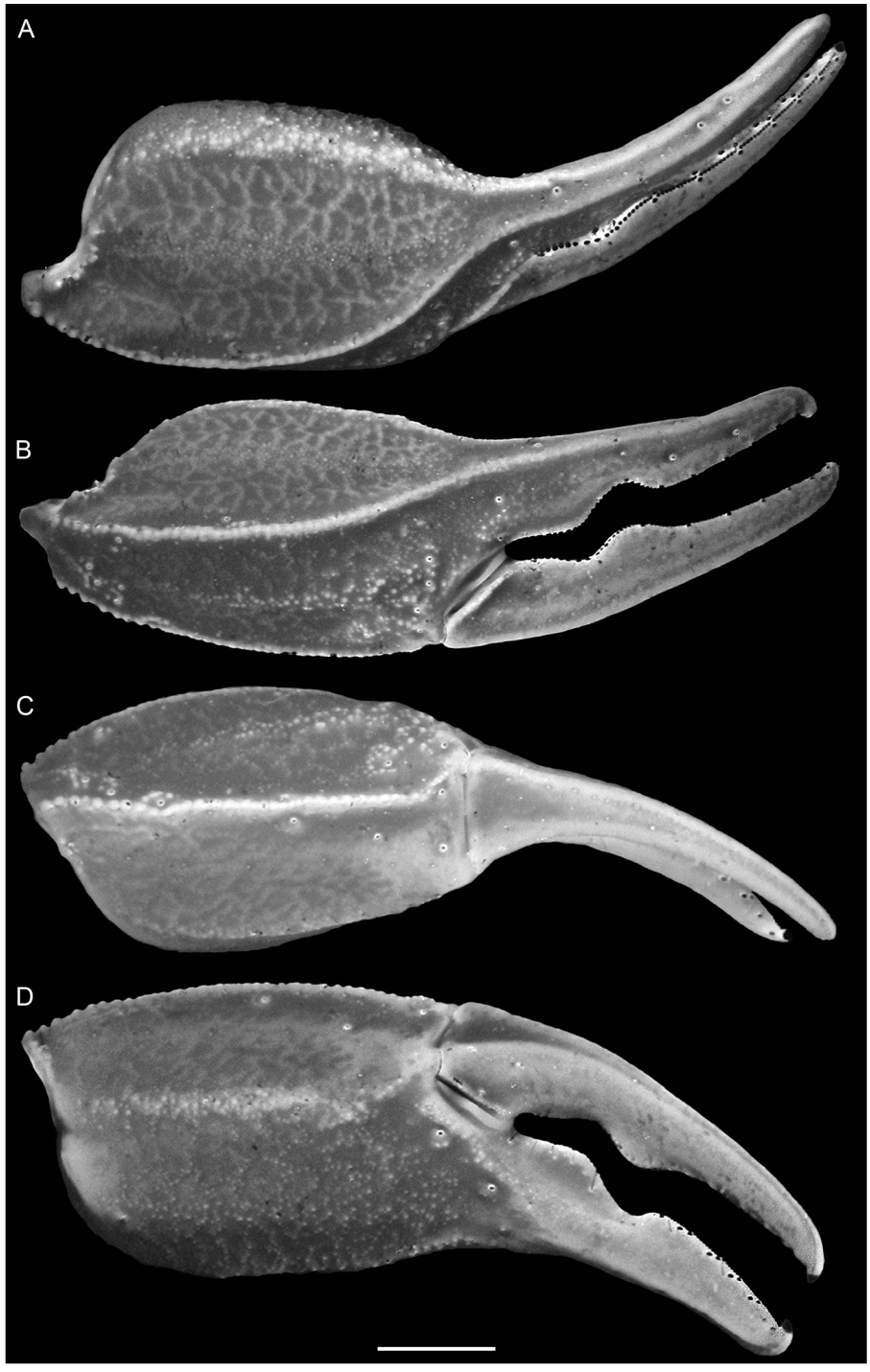

FIGURE 8. *Euscorpius olympus*, sp. nov., holotype ♂ (AMNH), dextral pedipalp chela, dorsal (**A**), retrolateral (**B**), ventral (**C**) and prolateral (**D**) aspects. Scale bar = 2 mm.

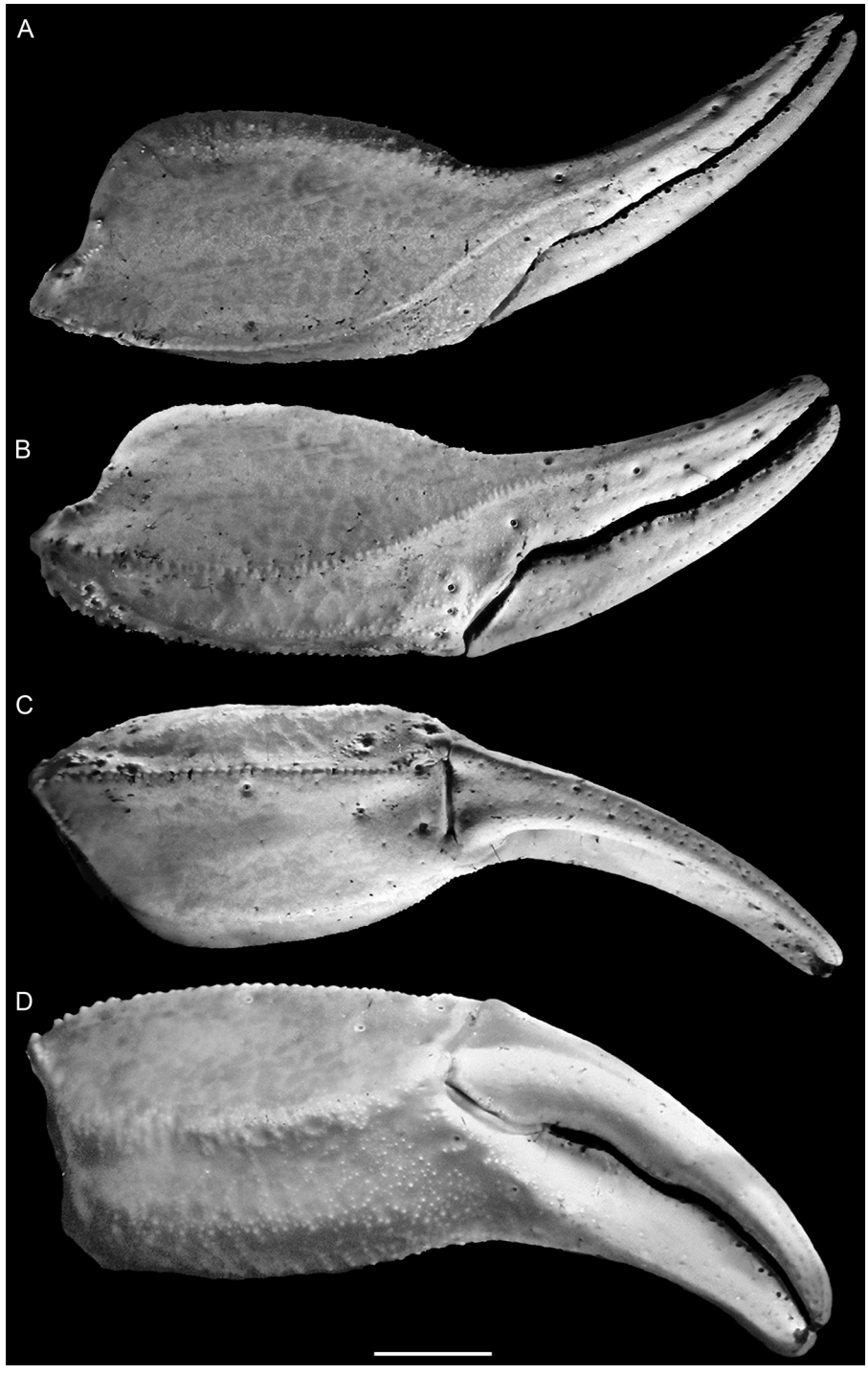

FIGURE 9. *Euscorpius olympus*, sp. nov., paratype ♀ (AMNH), dextral pedipalp chela, dorsal (**A**), retrolateral (**B**), ventral (**C**) and prolateral (**D**) aspects. Scale bar = 2 mm.

FIGURE 10. *Euscorpius olympus*, sp. nov., paratype ♀ (AMNH) dextral legs I–IV, basitarsi and telotarsi, proventral aspect (**A–D**). Scale bar = 1 mm.

tion proximally in *E. kinzelbachi* (fig. 19E); and the lobe almost completely circular in *E.* aff. *sicanus* (fig. 19F).

Etymology: The specific epithet is a name in apposition, referring to Mount Olympus, a legendary mountain in Greece where the type material was collected.

Description: The following description is based on the type material (see tables 2–4 for measurements and meristic data).

Total length: Medium sized, 45.5 mm (40.9–48.4 mm, *n* = 5) (♂) or 43.3 mm (38.2–46.7 mm, *n* = 5) (♀) (fig. 5; tables 2, 3).

Color: Mostly dark brown (fig. 3). Carapace darker, especially in female; posterior and posterolateral margins ochraceous. Pedipalps darker, especially in female. Legs slightly lighter brown, darker in female. Tergites dark brown, with posterior and lateral margins ochraceous. Telson vesicle ochraceous, darker, slightly reddish orange in female; with three longitudinal stripes in both sexes, one between anterodorsal sulci, the other pair along ventrolateral sulci; aculeus black.

Chelicerae: Manus, dorsal and retrolateral surfaces predominantly smooth, sparsely setose; prolateral and ventral surfaces densely setose (fig. 6A, B). Fixed finger, dorsal margin with four teeth: distal, subdistal, median and basal; distal and subdistal teeth well separated, median and basal fused into biscuspid. Movable finger, dorsal margin with five teeth: one prodistal, two subdistal, one median and one basal; prodistal (DI) and retrodistal (DE) teeth asymmetric, DI twice length of DE; median teeth large; basal teeth small.

Carapace: Carapace anterior width : posterior width, 59.9% (54.5–63.6%, *n* = 5) (♂) or 63.4% (61.1–66.1%, *n* = 5) (♀); posterior width of length, 94.3% (90.2–98.2%, *n* = 5) (♂) or 93.6% (88.1–96.9%, *n* = 5) (♀) (tables 2, 3). Carapace margin with shallow anteromedian notch; anteromedian sulcus distinct, narrow, fairly deep; posteromedian sulcus obsolete, shallow; posterolateral sulci shallow (fig. 6A, B). Interocular carina separating pair of median ocelli; three pairs of lateral ocelli, posterolateral major (PLMa), median lateral major (MLMa), and anterodorsal minor (ADMi); MLMa slightly larger than PLMa, both much larger than ADMi. Interocular surface finely granular (♂) to almost smooth (♀); lateral surfaces finely and sparsely granular; margins costate-granular. Carapace surfaces almost asetose; anterior margin with three to four microsetae; two microsetae situated posterior to median ocelli.

TABLE 4. Meristic data of *Euscorpius olympus*, sp. nov., type material, deposited in the American Museum of Natural History (AMNH), New York, including the Ambrose Monell Cryocollection for Molecular and Microbial Research (AMCC). Counts (sinistral/dextral) of median denticle subrows, prolateral accessory denticles (PAD) and retrolateral accessory denticles (RAD) on fixed and movable fingers of pedipalp chela; ventromedian spinules (VMS) on telotarsi of legs I–IV; and pectinal teeth.

		Holotype	Paratypes			
		♂	♂	♂	♂	♂
		AMNH	AMNH	AMNH	AMNH	AMNH
Pedipalp chela	fixed finger subrows	7/7	7/7	7/7	7/7	7/7
	fixed finger PAD	12/12	12/12	11/11	11/11	12/12
	fixed finger RAD	7/7	7/7	7/7	7/7	7/7
	movable finger subrows	7/7	7/7	7/7	7/7	7/7
	movable finger PAD	12/12	12/12	12/12	12/13	13/12
	movable finger RAD	7/7	7/7	7/7	7/7	7/7
Telotarsal VMS	leg I	11/11	9/10	10/10	-/11	11/10
	leg II	11/11	8/9	11/12	10/10	10/11
	leg III	13/13	11/10	10/10	11/10	11/13
	leg IV	12/12	10/10	11/11	12/12	13/13
Pectines	tooth count	8/8	9/8	8/8	8/8	8/8
		Paratypes				
		♀	♀	♀	♀	♀
		AMNH	AMNH	AMCC LP 17925	AMCC LP 17932	AMCC LP 17940
Pedipalp chela	fixed finger subrows	7/7	7/7	7/7	7/7	7/7
	fixed finger PAD	12/11	12/12	11/11	12/13	12/11
	fixed finger RAD	7/7	7/7	7/7	7/7	7/7
	movable finger subrows	7/7	7/7	7/7	7/7	7/7
	movable finger PAD	12/13	12/11	12/11	12/13	12/11
	movable finger RAD	7/7	7/7	7/7	7/8	8/7
Telotarsal VMS	leg I	10/-	11/11	11/11	11/11	11/11
	leg II	10/11	11/-	11/11	11/11	11/11
	leg III	11/10	12/12	11/11	11/13	-/12
	leg IV	12/12	13/12	13/12	12/12	10/12
Pectines	tooth count	7/7	7/7	7/7	7/7	7/7

Sternum: Subpentagonal (fig. 6C, D) with marked posterior depression. Surface with four or five macrosetae and few additional microsetae.

Pedipalps: Femur width of length, 32.7% (30.9–33.8%, $n = 5$) (♂) or 31.3% (29–32.8%, $n = 5$) (♀) (tables 2, 3). Proventral carina complete, costate-granular, with large subspiniform granules (fig. 7A, B, 16A). Promedian carina complete, costate-granular, spiniform granules

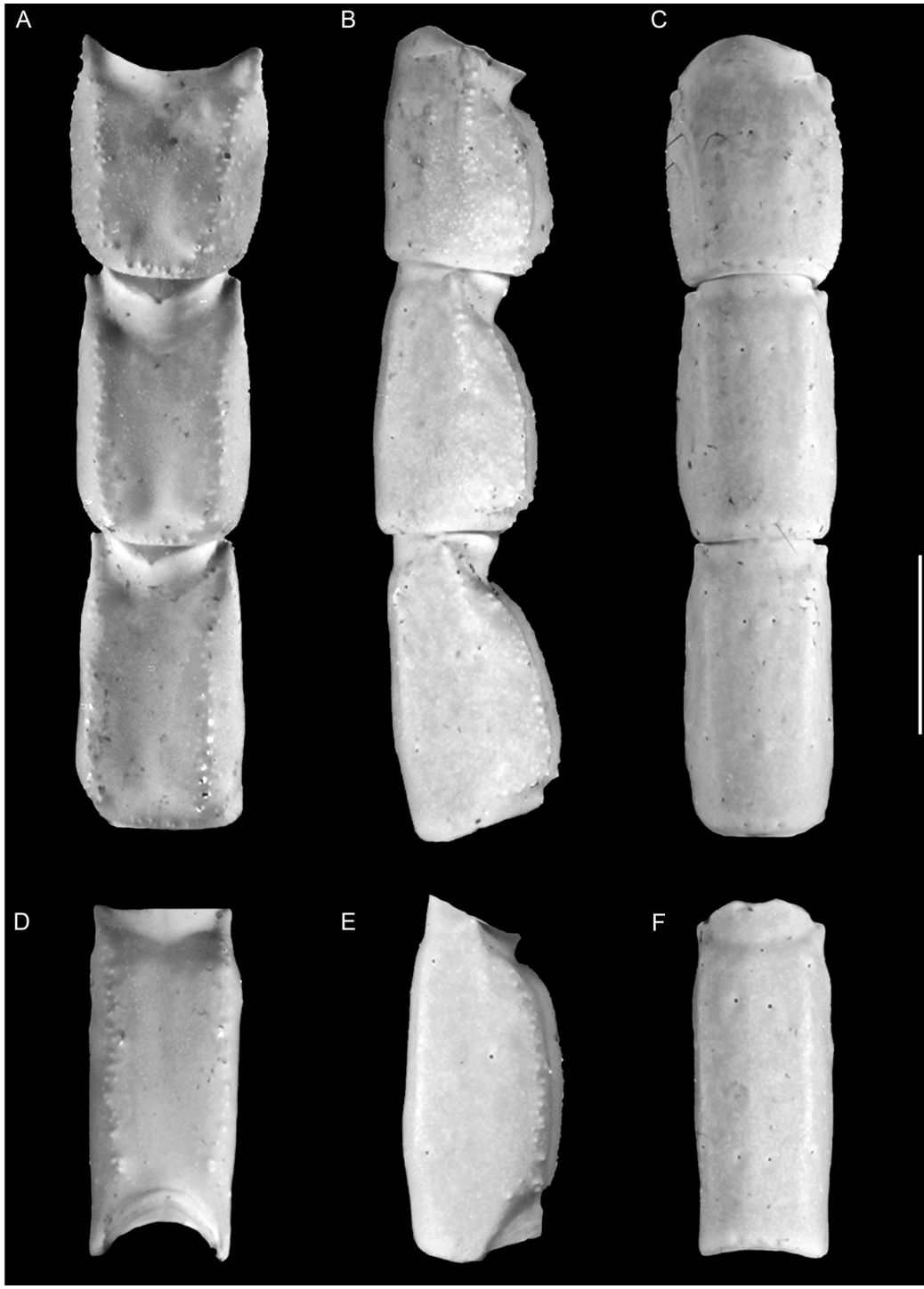

FIGURE 11. *Euscorpius olympus*, sp. nov., holotype ♂ (AMNH), metasomal segments I–IV, dorsal (**A, D**), lateral (**B, E**) and ventral (**C, F**) aspects. Scale bar = 2 mm.

FIGURE 12. *Euscorpius olympus*, sp. nov., paratype ♀ (AMNH), metasomal segments I–IV, dorsal (**A, D**), lateral (**B, E**) and ventral (**C, F**) aspects. Scale bar = 2 mm.

FIGURE 13. *Euscorpius olympus*, sp. nov., metasomal segment V, dorsal (**A, D**), lateral (**B, E**) and ventral (**C, F**) aspects. **A–C.** Holotype ♂ (AMNH). **D–F.** Paratype ♀ (AMNH). Scale bar = 2 mm.

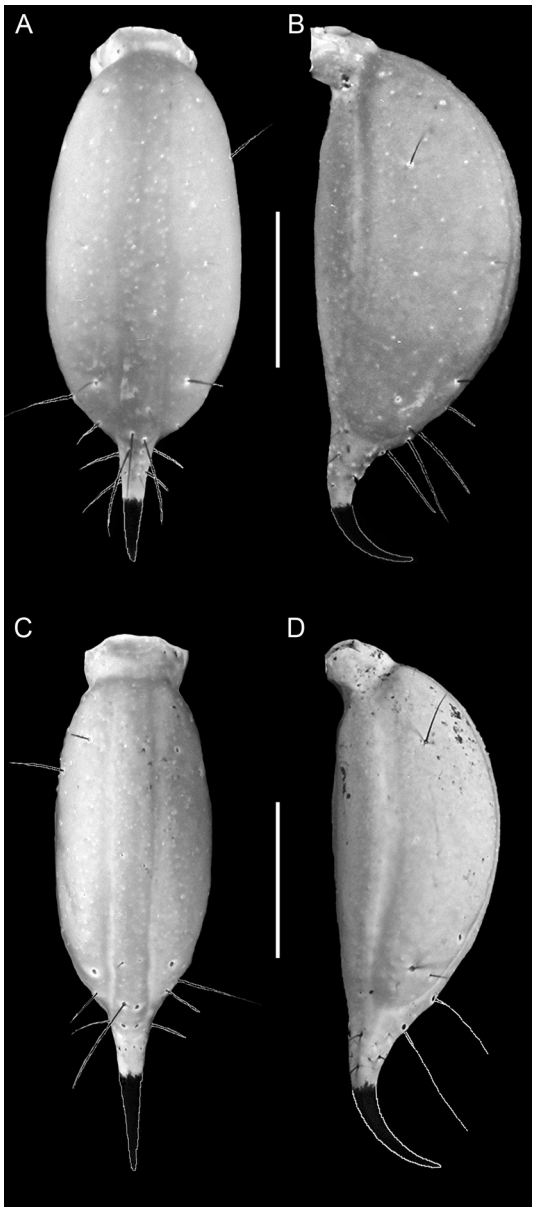

FIGURE 14. *Euscorpius olympus*, sp. nov., telson, ventral (**A, C**) and lateral (**B, D**) aspects. **A, B.** Holotype ♂ (AMNH). **C, D.** Paratype ♀ (AMNH). Scale bars = 2 mm.

more pronounced in ♂ than ♀, with few macro- and microsetae. Prodorsal carina complete, costate-granular, with several subspiniform granules. Retrodorsal carina complete, granular, becoming obsolete distally. Retromedian carinae complete, costate-granular, except at proximal and distal margins of segment, spiniform granules more pronounced in ♂ than ♀, and with few macro- and microsetae. Retroventral carina granular, restricted to proximal half of segment. Other carinae absent. Dorsal and ventral intercarinal surfaces finely granular; prolateral and retrolateral intercarinal surfaces smooth or nearly so.

Patella width of length, 37.8% (37.5–38.1%, n = 5) (♂) or 37.4% (34–39.9%, n = 5) (♀) (tables 2, 3). Proventral carina complete, granular to costate-granular, more pronounced in ♂ (fig. 7G) than ♀ (fig. 7H). Prodorsal carina complete, costate-granular, proportionally more developed than retrodorsal carina, and slightly more pronounced in ♂ (fig. 7C) than ♀ (fig. 7D). Retrodorsal and retroventral carinae complete, costate-granular (♂) (fig. 7C, E, G) or granular (♀) (fig. 7D, F, H), except at proximal and distal margins of segment. Retromedian carina incomplete, granular (fig. 7E, F). Other carinae absent. Dorsal and ventral intercarinal surfaces finely granular to smooth (fig. 7C, D, G, H); prolateral surface with distinct patellar process, finely granular, with few larger granules, more spiniform in ♂ (fig. 7C, G) than ♀ (fig. 7D, H), at base; surface of process with scattered microsetae and single macroseta near apex (fig. 7C, D, G, H); retrolateral intercarinal surface smooth (fig. 7E, F).

Chela slender, elongated, fingers notably curved, narrower in ♂ (fig. 8) than ♀ (fig. 9); chela length of manus width, 30.6% (29.4–31.7%, n = 5) (♂) or 29.6% (27.1–31.5%, n = 5) (♀); manus width of length, 53.5% (52.9–54.3%, n = 5) (♂) or 51.9% (50–53.8%, n = 5) (♀); manus height of width, 72.5% (67.5–76.2%, n = 5) (♂) or 64.1% (57.5–74.2%, n = 5) (♀); movable finger length : manus length, 92.1% (88.6–98.5%, n =

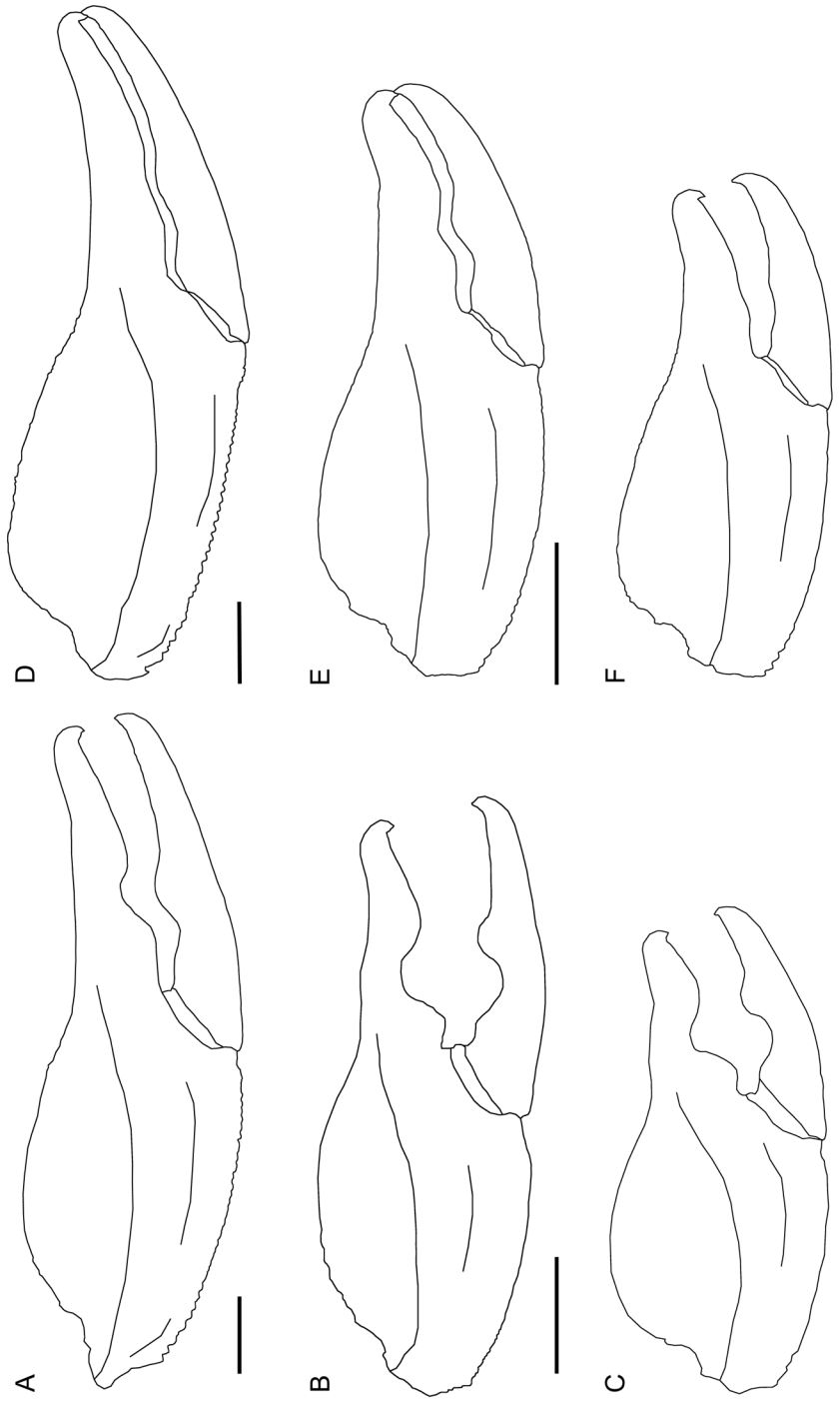

FIGURE 15. Shapes of pedipalp chela, retrolateral aspect of three species of *Euscorpius* Thorell, 1876, occurring in the vicinity of Mount Olympus, Greece. **A, D.** *Euscorpius olympus*, sp. nov., ♂ (**A**), ♀ (**D**). **B, E.** *Euscorpius kinzelbachi* Tropea et al., 2014, ♂ (**B**), ♀ (**E**). **C, F.** *Euscorpius* aff. *sicanus*, ♂ (**C**), ♀ (**F**). Scale bars = 2 mm.

5) (♂) or 90.6% (87–94.9%, *n* = 5) (♀); fixed finger width of length, 8.3% (6.9–10.3%, *n* = 5) (♂) and 8.9% (7.4–10%, *n* = 5) (♀); movable finger width of length, 4.8% (4.2–5.6%, *n* = 5) (♂) or 7.4%, (5.1–9.5%, *n* = 5) (♀) (tables 2, 3). Chela dorsal surface flat (♀) (fig. 9A, B) to slightly convex (♂) (fig. 8A, B), sloping slightly from proximal to distal margin (more so in ♀), proximal margin slightly curved; prolateral surface convex proximally, moderately (♀) (fig. 8D) to markedly (♂) (fig. 7D) concave distally (proximal to fixed finger); retrolateral surface slightly (♂) (fig. 8B) to markedly (♀) (fig. 9B) convex medially; ventral surface flat, sloping slightly from proximal to distal margin (more so in ♀), shallow depression proximal to movable finger condyle, proximal margin slightly curved (figs. 8C, 9C). Proventral carina obsolete, finely granular, more developed than ventromedian carina (figs. 8C, D, 9C, D). Promedian carina obsolete, finely granular, extending to base of fixed finger (figs. 8D, 9D). Prodorsal carina obsolete, granular, comprising discontinuous row of granules (figs. 8A, B, 9A, B). Dorsomedian carina obsolete, reduced to fine granulation along manus, absent on fixed finger (figs. 8A, B, 9A, B). Digital carina costate-granular to granular, incomplete, reduced to discontinuous row of subspiniform granules distally (figs. 8A, B, 9A, B). Subdigital carina vestigial, reduced to few granules at proximal margin of segment (figs. 8A, B, 9A, B). Retromedian carina incomplete, comprising obsolete row of granules decreasing in size distally (figs. 8B, C, 9B, C). Retrolateral secondary and secondary accessory carinae vestigial, reduced to distal quarter of segment, proximal to movable finger condyle (figs. 8B, C, 9B, C). Retroventral carina complete, costate-granular, comprising subspiniform granules (figs. 8B–D, 9B–D). Ventromedian carina obsolete, finely granular (figs. 8C, D, 9C, D). Intercarinal surfaces sparsely setose, smooth and glabrous to finely granulo-reticulate (figs. 8, 9). Fixed and movable fingers with pronounced proximal and medial lobes, respectively, and correspondingly deep proximal and medial notches in ♂ (fig. 8B, D); proximal and medial lobes both wider than high, but medial lobe higher and medial notch deeper; median lobe fits evenly with median notch, leaving little to no gap between fingers, when closed. Proximal and medial lobes, and corresponding notches, of fixed and movable fingers obsolete, shallow in ♀ (fig. 9B, D). Median denticle rows of fixed and movable fingers each comprising seven subrows (table 4), forming sublinear row, discontinuous at accessory denticles (figs. 8, 9); fixed and movable fingers each with 11–13 prolateral and 7 or 8 retrolateral accessory denticles (*n* = 10; table 4) and single terminal denticle, interlocking unevenly, movable finger moderately displaced retrolaterally, when closed (figs. 8, 9); intercarinal surfaces smooth, slightly setose (figs. 7, 8).

Femur with three trichobothria (figs. 7A, B, 16A), two on dorsal surface (d_1, d_2), one on prolateral surface (*i*). Patella with 35 or 36 trichobothria, one petite (esb_2), 34 or 35 full sized (figs. 7C–H, 16B, C, D): 9 or 10 on ventral surface (v_1–v_{10}); 24 on retrolateral surface (et_1–et_6, est_1–est_4, em_1–em_4, esb_1–esb_2, esb_{a1}–esb_{a4}, eb_1–eb_4); two on dorsal surface (d_1, d_2); and one on prolateral surface (*i*). Chela with 26 trichobothria, two petite (Et_4, *Esb*), 24 full sized (figs. 8, 9, 17A–D): 18 on manus, four on ventral surface (V_1–V_4), 10 on retrolateral surface (Et_1–Et_5, *Est*, *Esb*, Eb_1–Eb_3,), two on dorsal surface (*Dt*, *Db*), two on prolateral surface (*it, ib*); eight on fixed finger, four on dorsal surface (*dt*, *dst*, *dsb*, *db*), four on retrolateral surface (*et*, *est*, *esb*, *eb*).

Legs: Femora each with granular retrodorsal carina complete on legs II and III, incomplete, restricted to proximal three quarters, on I and IV, and costate-granular proventral carina complete

on I–III, incomplete, restricted to proximal three-quarters on IV, other carinae absent; prolateral and retrolateral surfaces finely granular; few macrosetae on carinae and other surfaces. Patellae each with granular retrodorsal carina on legs I–III, obsolete on IV, other carinae absent; few macrosetae on carina and other surfaces; pro- and retrolateral surfaces finely granular to smooth. Tibiae acarinate, each with few setiform macrosetae on pro- and retrolateral surfaces; tibial spur absent. Basitarsi acarinate; prolateral and retrolateral surfaces sparsely setose, more so on legs I and II than III and IV; distally with pro- and retrolateral pedal spurs, and proventral row of short, blunt spinules, 11 or 12 spinules on leg I, 3–5 on II and III, and 0–2 on IV (fig. 10). Telotarsi each with truncate laterodistal lobes and ventromedian row of short, blunt spinules; 8–11 spinules in ventromedian row on legs I and II, 10–13 on III and IV, last pair of spinules slightly elongated; ungues curved, equal in length; dactyl pronounced (fig. 10; table 4).

Genital operculum: Opercula suboval, separated longitudinally, slightly overlapping (♂) or partially fused (♀). Genital papillae well developed, protruding from below opercula (♂) (fig. 6C) or absent (♀) (fig. 6D).

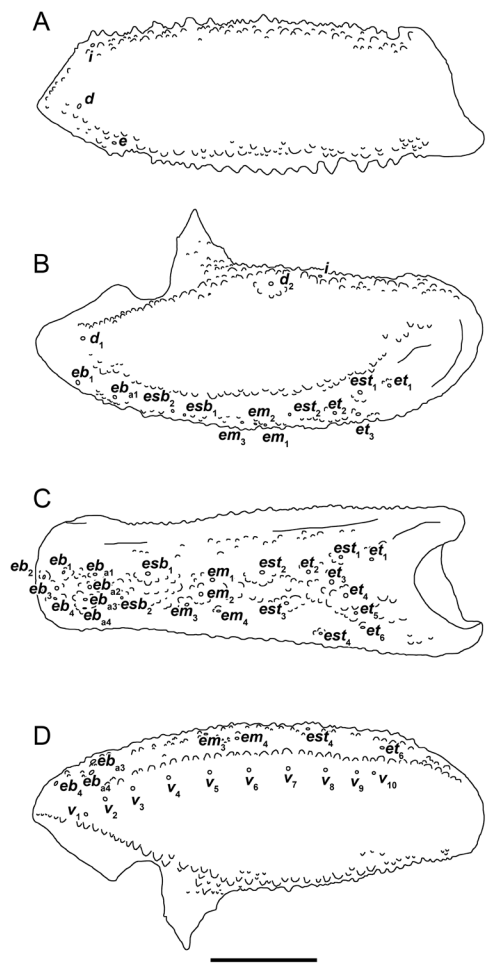

FIGURE 16. *Euscorpius olympus*, sp. nov., holotype ♂ (AMNH), dextral pedipalp femur, dorsal aspect (**A**) and patella, dorsal (**B**), retrolateral (**C**), and ventral (**D**) aspects, illustrating trichobothrial pattern. Annotations: *d*, dorsal; *e*, external; *eb*, external basal; *em*, external medial; *esb*, external suprabasal; *est*, external subterminal; *et*, external terminal; *i*, internal; *v*, ventral. Scale bar = 2 mm.

Hemispermatophore: Lamelliform (figs. 18, 19A). Flagellar lamina elongate, broad proximally and progressively tapering distally; dorsal and ventral margins weakly sclerotized; apex blunt, rounded (figs. 18, 19A). Capsule complex, divided into two similar parts (fig. 18A, D); two lateral lobes, one anterior to the other, each terminating in crownlike structure ("dorsal trough margin" sensu Sissom, 1994: 269–270; "tube-like structure" sensu Soleglad and Sissom, 2001: 56; figs 18C, 19A, D); posterior crownlike structure (*cls* 1) and anterior crownlike structure (*cls* 2) bearing ca. 13 and ca. 9 denticles, respectively (fig. 19D); two well-developed distal external lobes, posterior distal external lobe (*lde* 1) less pronounced than anterior distal external lobe (*lde* 2), which exhibits more rounded dorsal process (fig. 19D); two obsolete distal internal lobes; two well-developed basal lobes, posterior basal lobe (*bl* 1) terminating in tubular apex and larger than anterior basal lobe (*bl* 2), terminating acutely (fig. 19D). Trunk broad, unsclerotized, with distinct truncal flexure and short pedicel.

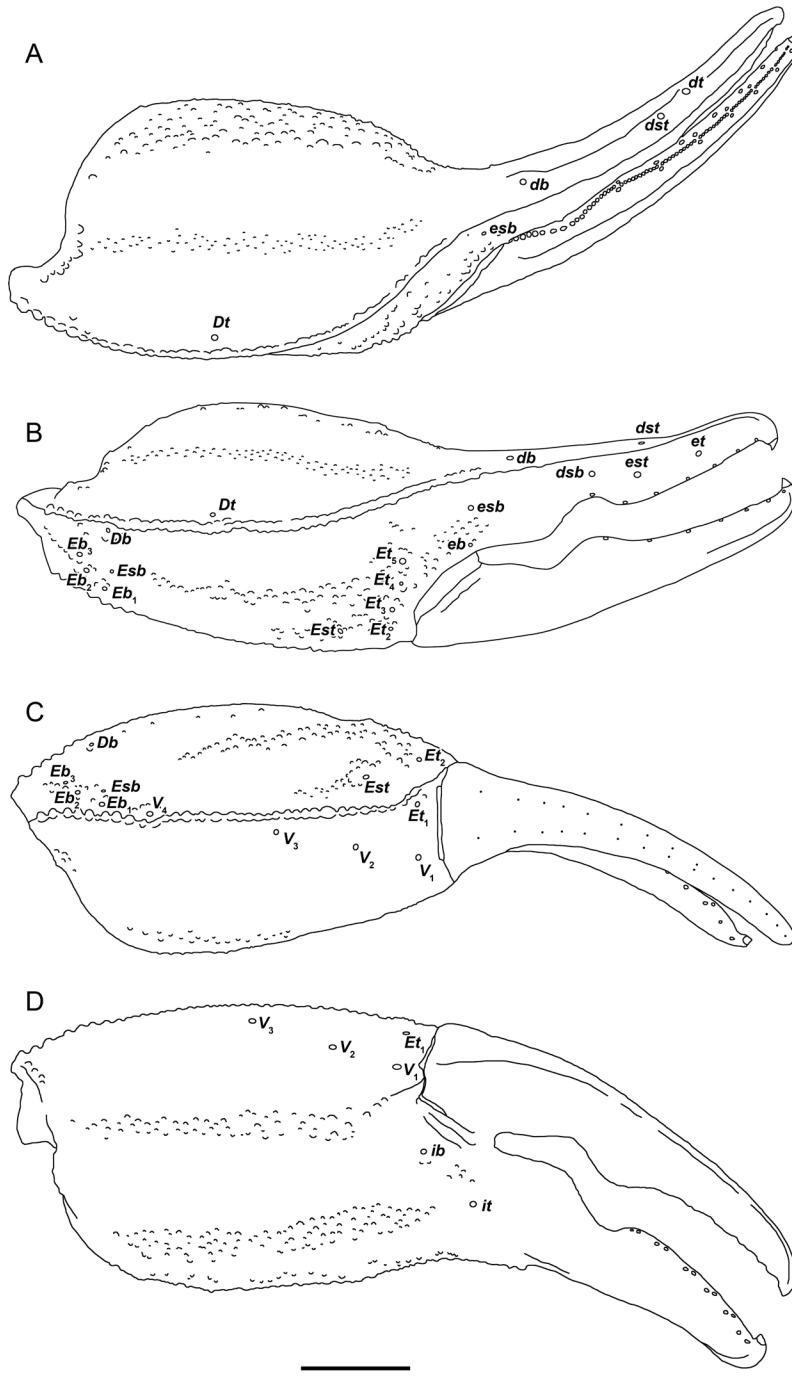

FIGURE 17. *Euscorpius olympus*, sp. nov., holotype ♂ (AMNH), dextral pedipalp chela, dorsal (**A**), retrolateral (**B**), ventral (**C**), and prolateral (**D**) aspects, illustrating trichobothrial pattern. Annotations: *Db*, *db*, dorsal basal; *dsb*, dorsal suprabasal; *dst*, dorsal subterminal; *Dt*, *dt*, dorsal terminal; *Eb*, *eb*, external basal; *Esb*, *esb*, external suprabasal; *Est*, *est*, external subterminal; *et*, *Et*, external terminal; *ib*, internal basal; *it*, internal terminal; *V*, ventral. Scale bar = 2 mm.

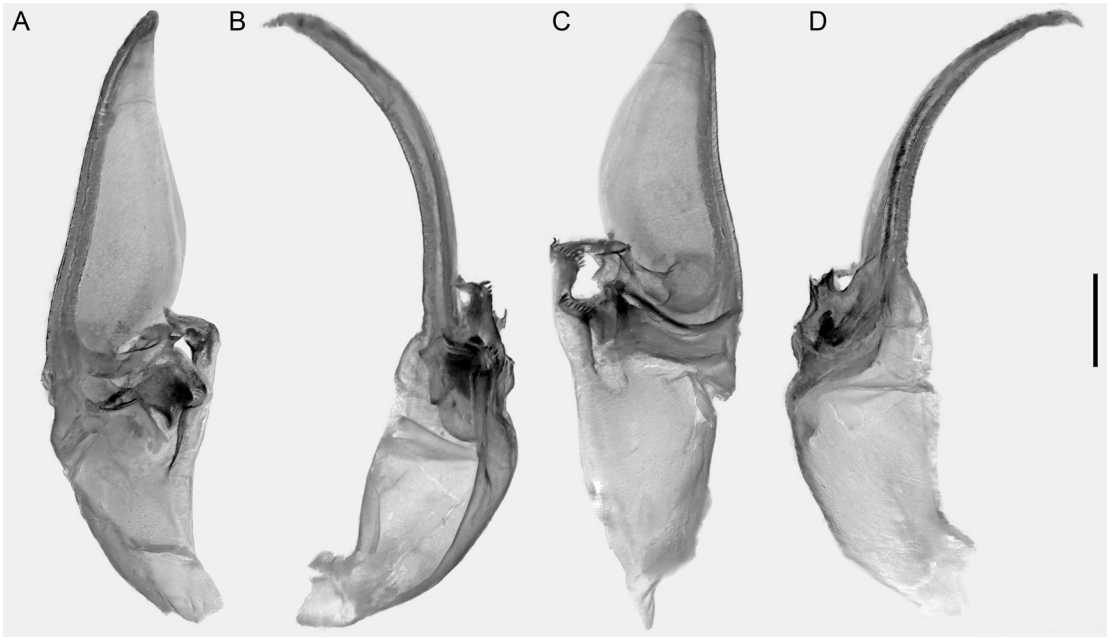

FIGURE 18. *Euscorpius olympus*, sp. nov., paratype ♂ (AMNH), sinistral hemispermatophore. **A.** Ental aspect. **B.** Dorsal aspect. **C.** Ectal aspect. **D.** Ventral aspect. Scale bars: 1 mm.

Pectines: Pectinal tooth count, 8/8 (n = 5) (♂) or 7/7 (n = 5) (♀). Surfaces with macro- and microsetae, mostly on marginal lamellae. Basal plate anvil shaped, with moderate (♀) (fig. 6D) to pronounced (♂) (fig. 6C) anteromedian invagination.

Tergites: Pretergites and posttergites progressively increasing in length. Pretergites glabrous; posttergites III–VII finely and densely (♂) or sparsely (♀) granular submedially and along posterior margins, more coarsely so on VII, especially in ♂; posttergites III–VII each with obsolete dorsomedian carinae.

Sternites: Sternites III–VII surfaces smooth and sparsely setose medially, finely granular (♂) or smooth (♀), each with 10–12 microsetae, along lateral and posterior margins; III–VI each with pair of oval-shaped spiracles sublaterally; VII with obsolete ventrolateral and ventrosubmedian carinae.

Metasoma: Segments I–V narrow and slender, progressively increasing in length and decreasing in width (tables 2, 3). Dorsolateral carinae obsolete, granular on segments I and II (figs. 11A, B, 12A, B); granular to costate-granular posteriorly, posterodorsal granules slightly larger than preceding granules on III and IV (figs. 11A, B, D, E, 12A, B, D, E); granular on V (fig. 13A, B, D, E). Median lateral carinae obsolete, reduced to few granules in anterior half of segment I; reduced to few granules in anterior half or absent on II; absent on III–V (figs. 11B, 12B). Ventrolateral carinae absent or obsolete on segments I–IV (figs. 11B, C, E, F, 12B, C, E, F); distinct, costate-granular, with spiniform granules on V, but incomplete posteriorly, granules not reaching anal lobes (fig. 13B, C, E, F). Ventromedian carinae absent on segments I–IV (figs. 11C, F, 12C, F); distinct, but incomplete on V (fig. 13C, F). Anal arch of segment V with 12 ventral lobes, two lateral lobes on each side and rounded

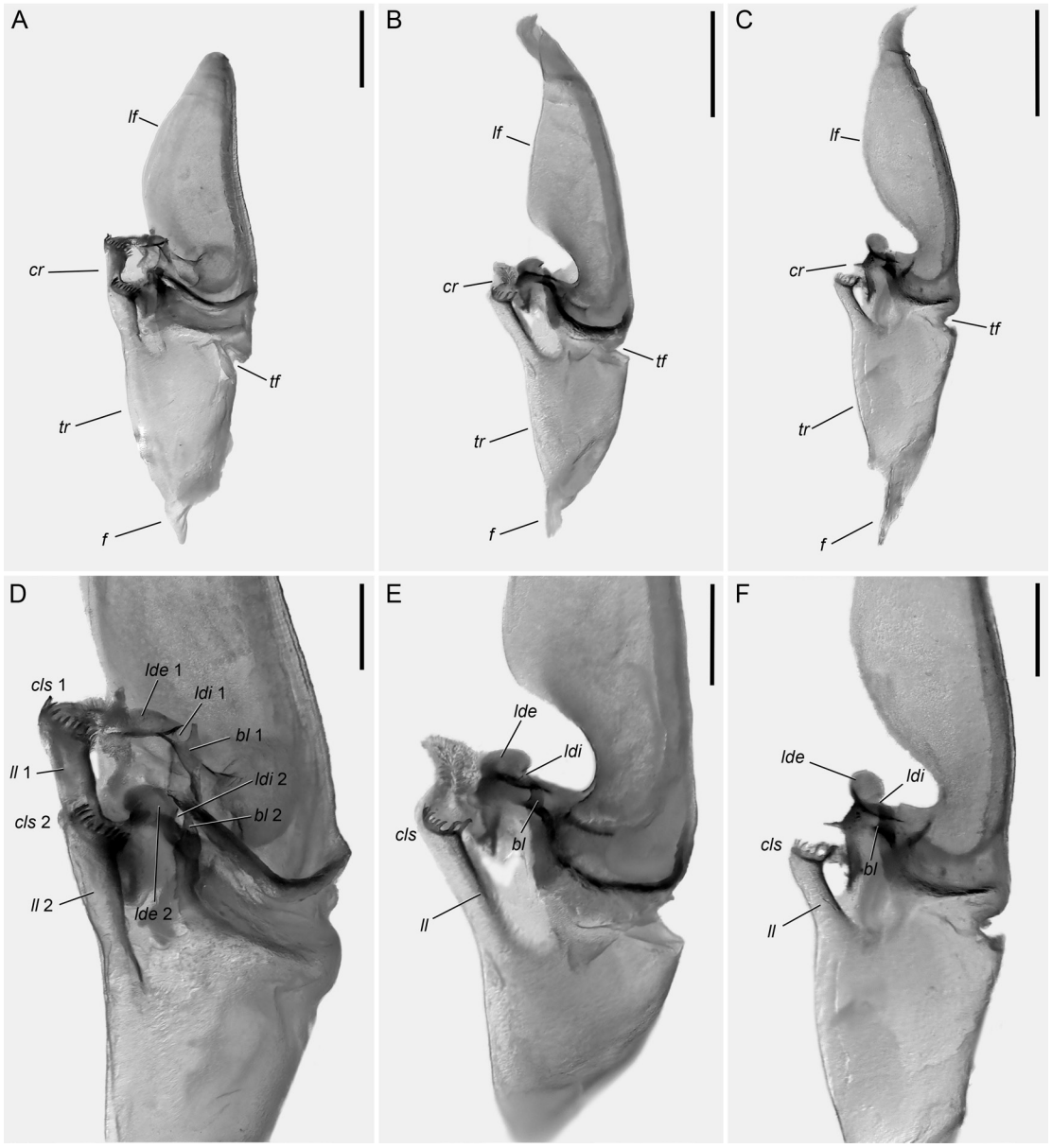

FIGURE 19. Sinistral hemispermatophores of three species of *Euscorpius* Thorell, 1876, occurring in vicinity of Mount Olympus, Greece, ectal aspect (**A–C**) and detail of capsular region (**D–F**). **A, D.** *Euscorpius olympus*, sp. nov., paratype ♂ (AMNH). **B, E.** *Euscorpius kinzelbachi* Tropea et al., 2014, ♂ (AMNH). **C, F.** *Euscorpius* aff. *sicanus*, ♂ (AMNH). Annotations: *fl*, flagellar lamina; *f*, foot; *cr*, capsule region; *tf*, truncal flexure; *tr*, trunk; *cls*, crown-like structure; *ll*, lateral lobe; *lde*, distal external lobe; *ldi*, distal internal lobe; *bl*, basal lobe. Scale bars = 1 mm (**A–C**); scale bars = 0.5 mm (**D–F**).

dorsal depression (fig. 13). Dorsal intercarinal surfaces finely granular on segments I–V (figs. 11A, D, 12A, D, 13A, D); retrolateral intercarinal surfaces finely granular on I and V (figs. 11B, 12B, 13B, E), smooth on II–IV (figs. 11B, E, 12B, E); ventral intercarinal surfaces smooth on I–IV (figs. 11C, F, 12C, F), finely granular on V (fig. 13C, F). Macrosetae arranged in groups of 8–9 per segment (figs. 11, 12), with more setae on segment V (fig. 13).

Telson: Vesicle globose, shallowly convex ventrally, more so in ♂ (fig. 14); pairs of anterodorsal, ventrolateral, and ventrosubmedian longitudinal sulci; surfaces smooth, with scattered macro- and microsetae anterior to aculeus. Aculeus short, curved, forming acute (♂) or obtuse (♀) angle with vesicle (fig. 14B, D); approximately one third (♂) to half (♀) the length of vesicle (tables 2, 3).

Distribution: *Euscorpius olympus*, sp. nov., is known only from the type locality, Foteina, in the foothills of Mount Olympus, Central Macedonia, Greece (figs. 1B, 2B, 4B).

Ecology: The type specimens of *E. olympus*, sp. nov., were collected at night on a deciduous forest slope, from deep, narrow crevices in limestone outcrops (fig. 4B). The habitat and habitus of this species are consistent with the lithophilous ecomorphotype (Prendini, 2001).

Euscorpius olympus is sympatric with two other euscorpiids, a species of the *E. sicanus* complex that lives primarily among the leaf litter, and *E. kinzelbachi*, a montane species inhabiting pine forests mostly at higher elevations across Mount Olympus. A buthid, *Mesobuthus gibbosus* (Brullé, 1832), has been recorded in drier, rocky habitats at lower elevations, around the massif.

DISCUSSION

The description of *E. olympus*, sp. nov., raises the number of species in *Euscorpius* to 74 across its distribution and to 32 in Greece (Parmakelis et al., 2013; Fet et al., 2016, 2018; Podnar et al., 2021; Tropea et al., 2022; Kovařík et al., 2023; table 1). Greece appears to be one of the centers of origin and diversification for *Euscorpius*. Lineage divergences suggest that the clades of Aegean *Euscorpius* diversified approximately 2.5–10 Mya, between the late Miocene and early Pleistocene (Parmakelis et al., 2013). Fragmentation of the Aegeid plate, the Messinian reemergence of land bridges, Pliocene regression of the Aegean region and later on, Pleistocene sea level fluctuations, appear to have driven the diversification of *Euscorpius* in the Aegean islands, as in other co-distributed taxa (Çiplak et al., 2010). Patterns of speciation among *Euscorpius* on the Greek mainland were less obvious (Parmakelis et al., 2013; Fet et al., 2018) until Podnar et al. (2021) shed some light on the evolutionary relationships and time divergences among Balkan *Euscorpius*. Miocene-Pliocene origins were suggested for most of the species, including those on the Greek mainland, with the Middle Miocene Climate Transition (MMCT) and the Messinian Salinity Crisis (MSC) having played important roles in the major diversification events. But how did events in the Pleistocene, which structured the genetics and distributions of current European biota (Hewitt, 1999, 2000, 2004; Schmitt, 2007) affect *Euscorpius* in Greece and specifically, the area around Mount Olympus?

Two of the *Euscorpius* species occurring around Mount Olympus, *E. kinzelbachi* and *E.* aff. *sicanus*, evidently followed different evolutionary pathways. The main divergence between the clades to which these species belong, occurred around 9.9 Mya (Messinian, Miocene). How-

ever, subsequent divergence from their respective sister species occurred around 3.2 Mya for *E. kinzelbachi* and 2.5 Mya for *E.* aff. *sicanus* (Podnar et al., 2021), during the Pliocene-Pleistocene. Microallopatry was suggested as a possible explanation for current species distributions across mainland Greece (Parmakelis et al., 2013), as in montane scorpions inhabiting other parts of the world. For example, orographic heterogeneity, associated with marked climatic variation, has been suggested to explain the high genetic diversity of *Buthus* Leach, 1815, scorpions in the Atlas Mountains of Morocco (Habel et al., 2012; Klesser et al., 2021).

In Greece, the orogeny of ranges such as Mount Olympus occurred during the Neogene, with some uplift and faulting continuing during the Pliocene and Pleistocene (Skilodimou et al., 2014). The occurrence of *E. kinzelbachi* in relictual forest patches of *Pinus heldreichii* Christ, 1863 (Podnar et al., 2021), at high altitudes on Mount Olympus (Theodoropoulos et al., 2011; Saladin et al., 2017) suggests that these forests acted as refugia during the MMCT and the Pliocene-Pleistocene glacial cycles (Smith et al., 1997; Leontaritis et al. 2020). Isolation in and specialization to habitat refugia may have resulted in the speciation of *E. kinzelbachi*. A similar process might be hypothesized on nearby Mount Ossa, where *Euscorpius ossae* Fet et al., 2013, the sister species of *E. kinzelbachi*, occurs. The mountain range that includes Mount Olympus and Mount Ossa is considered a glacial refugium (fig. 1C; Hewitt, 2004; Schmitt, 2007; Médail and Diadema, 2009), which probably allowed scorpion populations to survive during unfavorable glacial periods, and to colonize other areas during more favorable interglacial periods.

Euscorpius aff. *sicanus* is more widespread than the other two species, occurring across most of eastern Greece (i.e., Thessaly, including Mount Olympus, Mount Ossa, and Mount Pelion) and parts of central Greece (e.g., Tsaritsani), generally at lower, warmer elevations. This distribution, along with its genetic affinities with other species in western Greece (Fet et al., 2018) and Italy (Podnar et al., 2021), suggests a scenario of early population expansion during interglacial-glacial cycles. An estimate for the divergence of *E.* aff. *sicanus* falls within the Pliocene-Pleistocene transition, a period with glaciations and sea level fluctuations (2.5 Mya). As the sister species of *E.* aff. *sicanus* appears to belong to part of the *E. sicanus* complex occurring in Italy (Podnar et al., 2021), land bridges connecting the Italian and Balkan peninsulas presumably enabled gene flow before becoming submerged. More evidence for this ancient connection includes populations of the *E. sicanus* complex across the Greek mainland and offshore islands (Fet et al., 2018) and the presence of *Euscorpius garganicus* Caporiacco, 1950, a species widespread around southeastern Italy, on Palagruža island and the Tremiti islands in the Tyrrhenian Sea (Tropea, 2017), suggesting these islands provided stepping stones for dispersal. Pleistocene origins have also been suggested for other species such as *Euscorpius solegladi* Fet et al., 2014, which occurs near Mount Olympus in Greece and Bulgaria, and is phylogenetically related to *Euscorpius hadzii* Caporiacco, 1950, a complex of species widespread across the western Balkans (Fet et al., 2014).

The phylogenetic affinities of *E. olympus* remain to be tested. However, considering the profound morphological differences between this species and other congeners in the vicinity, its divergence is probably more ancient, and may have occurred well before the Pleistocene. The ancestral population of this species may have been isolated in lower elevation deciduous forests, inhabiting deep rock crevices during unfavorable climatic periods, and ultimately speciating in isolation.

In addition to historical factors, scorpion diversity and distribution are profoundly influenced by ecological factors such as humidity and temperature, which are often exacerbated by altitudinal zonation (Prendini and Bird, 2008; Habel et al., 2012; Klesser et al., 2021; Foord et al., 2015). Four main forest zones occur on Mount Olympus (Theodoropoulos et al., 2011): (1) the eumediterranean zone, comprising evergreen oak trees and shrubs, between 200–800 m; (2) the paramediterranean zone, comprising deciduous oak or mixed trees, e.g., *Platanus orientalis* L., 1753, at elevations between 270–500 m; (3) the mountainous and Mediterranean-conifer zone, comprising beech and fir trees, between 500–1700 m; and (4) the cold-adapted conifer zone, comprising pine and spruce, between 1700–2500 m. Such marked altitudinal zonation, mostly separated by barren plateaus and ridges, creates "sky islands" that isolate patches of fauna and flora across the landscape. The distributions of the three species of *Euscorpius* are associated with some of these unique zones, suggesting that habitat preferences restricted them to particular altitudes. The lithophilous *E. olympus* was only found in the crevices of large limestone outcrops in a paramediterranean deciduous forest patch at around 500 m. The corticolous/lapidicolous *E. kinzelbachi* appears to be restricted to pine forests in both the Mediterranean conifer and cold-adapted conifer zones, where it may be found under bark or rocks, from 500 to 2000 m. The lapidicolous *E.* aff. *sicanus* was found either under stones in arid rocky areas of the eumediterreanean zone or in the leaf litter of deciduous forests in the paramediterranean and mountainous zones, from 400 to 1000 m.

Euscorpius olympus appears to be the most stenotopic of the three species, given its restricted distribution and distinct microhabitat. Furthermore, the new species exhibits more pronounced ecomorphological adaptations than other sympatric congeners: marked dorsoventral compression, elongation of the pedipalp chelae, and short, blunt spinules in the ventromedian rows of the telotarsi, together with markedly curved ungues (Prendini, 2001). These traits are also exaggerated in other lithophilous and troglophilous species of the genus such as *E. aquilejensis*, *Euscorpius biokovensis* Tropea and Ozimec, 2020, and *Euscorpius feti* Tropea, 2013 (Tropea, 2013a, 2013b; Tropea and Ozimec, 2020). Isolation in rocky habitats during glacial periods might have enhanced the associated ecomorphological adaptations and driven scorpion diversification through niche divergence.

ACKNOWLEDGMENTS

Material was collected on scientific research permit ΥΠΕΝ/ΔΔΔ/8574/314 from the Ministry of Environment and Energy and the General Secretariat of Forests and Wildlife Management of the Republic of Greece. Fieldwork was supported by grant DEB 1655050 from the U.S. National Science Foundation to the second author (L.P.). The first author (J.B-A.) was supported by student scholarship 2021.04967.BD from the Fundação para Ciência e Tecnologia, Portugal. The authors thank the following: Stephan Schaffrath (formerly, University of Cologne, Germany) for collecting the first specimen of the new species; Arnau Calatayud-Mascarell (University of Idaho, Moscow) for assisting J.B.-A. in the field; Leonidas-Romanos Davranoglou (Oxford University) for assistance with collecting permits; Barbara Green (AMNH) for assisting J.B.-A. with a U.S. visa; James M. Carpenter (AMNH) for access to the Division of

Invertebrate Zoology; Pio A. Colmenares (AMNH) for logistical assistance and constructive suggestions; Jairo A. Moreno-González (AMNH) for taxonomic advice, assistance with hemispermatophore dissections and preparations, and comments on the manuscript; Steve Thurston (AMNH) for training J.B.-A. on the Microptics imaging system and assistance with the figures for this contribution; Mario García París and Alberto Sánchez Vialas (Museo Nacional de Ciencias Naturales de Madrid) and Javier Diéguez Uribeondo (Real Jardín Botánico de Madrid) for providing some collecting supplies; Emilio Blasco and Juana María Aróstegui for assistance with shipping and organization of the fieldwork materials; and Stephanie F. Loria (Zoologisches Museum, Universität Hamburg) and Leonidas-Romanos Davranoglou for constructive comments on the manuscript. This contribution is dedicated to the memory of Pedro Piquet for unconditional support and hospitality during several field trips by the first author.

REFERENCES

Baselga, A. 2008. Determinants of species richness, endemism and turnover in European longhorn beetles. Ecography 31: 263–271.

Blondel, J., J. Aronson, J.-Y. Bodiou, and G. Boeuf. 2010. The Mediterranean region: biological diversity in space and time. Oxford: Oxford University Press.

Caporiacco, L. di. 1950. Le specie e sottospecie del genre "*Euscorpius*" viventi in Italia ed in alcune zone confinanti. Memorie/Accademia Nazionale dei Lincei (serie VIII) 2: 159–230.

Çiplak, B., K.-G. Heller, and F. Willemse. 2010. Phylogeny and biogeography *Eupholidoptera* Mařan (Orthoptera, Tettigoniidae): Morphological speciation in correlation with the geographical evolution of the eastern Mediterranean. Systematic Entomology 35: 722–738.

Coope, G.R. 1994. The response of insect faunas to glacial-interglacial climatic fluctuations. Philosophical Transactions of the Royal Society of London B, Biological Sciences 344: 19–26.

Costa, G.J., et al. 2023. The effect of the Messinian salinity crisis on the early diversification of the *Tettigettalna* cicadas. Zoologica Scripta 52: 100–116.

Cuttelod, A.N. García, D.A. Malak, H.J. Temple, and V. Katariya. 2009. The Mediterranean: a biodiversity hotspot under threat. *In* J.-C. Vié, C. Hilton-Taylor, and S.N. Stuart (editors), Wildlife in a changing world – an analysis of the 2008 IUCN Red List of Threatened Species: 89–101. Gland, Switzerland: International Union for the Conservation of Nature (IUCN).

Drovetski, S.V., et al. 2018. A test of the European Pleistocene refugial paradigm, using a Western Palaearctic endemic bird species. Proceedings of the Royal Society of London B, Biological Sciences 285: 20181606.

Fet, V., and M.E. Soleglad. 2002. Morphology analysis supports presence of more than one species in the "*Euscorpius carpathicus*" complex (Scorpiones: Euscorpiidae). Euscorpius 3: 1–51.

Fet, V., M.R. Graham, M.M. Webber, and G. Blagoev. 2014. Two new species of *Euscorpius* (Scorpiones: Euscorpiidae) from Bulgaria, Serbia, and Greece. Zootaxa 3894: 83–105.

Fet, V., M.R. Graham, G. Blagoev, A. Karataş, and A. Karataş. 2016. DNA barcoding indicates hidden diversity of *Euscorpius* (Scorpiones: Euscorpiidae) in Turkey. Euscorpius 216: 1–12.

Fet, V., et al. 2018. Fauna and zoogeography of scorpions in Greece. *In* S. Sfenthourakis, P. Pafilis, A. Parmakelis, N. Poulakakis, and K. Triantis, Biogeography and biodiversity of the Aegean. In honour of Prof. Moysis Mylonas: 123–134. Nicosia: Broken Hill Publishers.

Foord, S.H., V. Gelebe, and L. Prendini. 2015. Effects of aspect and altitude on scorpion diversity along an environmental gradient in the Soutpansberg, South Africa. Journal of Arid Environments 113: 114–120.

Habel, J.C., et al. 2012. Microallopatry caused strong diversification in *Buthus* scorpions (Scorpiones: Buthidae) in the Atlas Mountains (NW Africa). PLoS One 7: e29403.

Hewitt, G.M. 1996. Some genetic consequences of ice ages, and their role in divergence and speciation. Biological Journal of the Linnean Society 58: 247–276.

Hewitt, G.M. 1999. Post-glacial re-colonization of European biota. Biological Journal of the Linnean Society 68: 87–112.

Hewitt, G.M. 2000. The genetic legacy of the Quaternary ice ages. Nature 405: 907–913.

Hewitt, G.M. 2004. Genetic consequences of climatic oscillations in the Quaternary. Philosophical Transactions of the Royal Society of London B, Biological Sciences 359: 183–195.

Klesser, R., et al. 2021. Molecular biogeography of the Mediterranean *Buthus* species complex (Scorpiones: Buthidae) at its southern Palaearctic margin. Biological Journal of the Linnean Society 133: 166–178.

Kovařík, F., G. Lowe, M. Byronová, and F. Šťáhlavský. 2020. *Euscorpius thracicus* sp. n. (Scorpiones: Euscorpiidae) from Bulgaria. Euscorpius 326: 1–17.

Kovařík, F., M. Audy, S.M. Sarbu, and V. Fet. 2023. *Euscorpius sulfur* sp. n. (Scorpiones: Euscorpiidae), a new cave scorpion from Albania and northwestern Greece. *Euscorpius* 376: 1–14.

Laurie, M. 1896. Further notes on the anatomy and development of scorpions, and their bearing on the classification of the order. Journal of Natural History 17: 121–133.

Leontaritis, A.D., K. Kouli, and K. Pavlopoulos. 2020. The glacial history of Greece: a comprehensive review. Mediterranean Geoscience Reviews 2: 65–90.

Loria, S.F., and L. Prendini. 2014. Homology of the lateral eyes of Scorpiones: a six-ocellus model. PLoS One 9: e112913.

Mauries, J.-P. 2003. *Schizmohetera olympica* sp. n. from Greece, with a reclassification of the superfamily Neoatractosomatoidea (Diplopoda: Chordeumatida). Arthropoda Selecta 12: 9–16.

Médail, F., and K. Diadema. 2009. Glacial refugia influence plant diversity patterns in the Mediterranean Basin. Journal of Biogeography 36: 1333–1345.

Minachilis, K., et al. 2020. Bumblebee diversity and pollination networks along the elevation gradient of Mount Olympus, Greece. Diversity and Distributions 26: 1566–1581.

Minachilis, K., et al. 2023. High species turnover and unique plant-pollinator interactions make a hyperdiverse mountain. Journal of Animal Ecology 92: 1001–1015.

Ochoa, J.A., R. Botero-Trujillo, and L. Prendini. 2010. On the troglomorphic scorpion *Troglotayosicus humiculum* (Scorpiones, Troglotayosicidae), with first description of the adults. American Museum Novitates 3691: 1–19.

Parmakelis, A., P. Kotsakiozi, I. Stathi, S. Poulikarakou, and V. Fet. 2013. Hidden diversity of *Euscorpius* (Scorpiones: Euscorpiidae) in Greece revealed by multilocus species-delimitation approaches. Biological Journal of the Linnean Society 110: 728–748.

Platania, L., M. Pavlek, and M. Arnedo. 2020. Testing the monophyly of the ground-dweller spider genus *Harpactea* Bristowe, 1939 (Araneae, Dysderidae) with the description of three new species. Systematics and Biodiversity 18: 688–707.

Podnar, M., I. Grbac, N. Tvrtković, C. Hörweg, and E. Haring. 2021. Hidden diversity, ancient divergences, and tentative Pleistocene microrefugia of European scorpions (Euscorpiidae: Euscorpiinae) in the eastern Adriatic region. Journal of Zoological Systematics and Evolutionary Research 59: 1824–1849.

Podnar, M., et al. 2022. *Alpiscorpius liburnicus* sp. n. with a note on the "*Alpiscorpius croaticus* group" (Scorpiones: Euscorpiidae) in Croatia. Natura Croatica: Periodicum Musei Historiae Naturalis Croatici 31: 265–282.

Prendini, L. 2000. Phylogeny and classification of the superfamily Scorpionoidea Latreille 1802 (Chelicerata, Scorpiones): an exemplar approach. Cladistics 16: 1–78.

Prendini, L. 2001. Substratum specialization and speciation in southern African scorpions: the Effect Hypothesis revisited. *In* V. Fet and P.A. Selden (editors), Scorpions 2001: in memoriam Gary A. Polis: 113–138. Burnham Beeches, Bucks, U.K.: British Arachnological Society.

Prendini, L. 2004. The systematics of southern African *Parabuthus* Pocock (Scorpiones: Buthidae): revisions to the taxonomy and key to the species. Journal of Arachnology 32: 109–186.

Prendini, L., and T.L. Bird. 2008. Scorpions of the Brandberg Massif, Namibia: species richness inversely correlated with altitude. African Invertebrates 49: 77–107.

Prendini, L., T.M. Crowe, and W.C. Wheeler. 2003. Systematics and biogeography of the family Scorpionidae (Chelicerata: Scorpiones), with a discussion on phylogenetic methods. Invertebrate Systematics 17: 185–259.

Prendini, L., and S.F. Loria, S.F. 2020. Systematic revision of the Asian forest scorpions (Heterometrinae Simon, 1879), revised suprageneric classification of Scorpionidae Latreille, 1802, and revalidation of Rugodentidae Bastawade et al., 2005. Bulletin of the American Museum of Natural History 442: 1–480.

Saladin, B., et al. 2017. Fossils matter: improved estimates of divergence times in *Pinus* reveal older diversification. BMC Evolutionary Biology 17: 1–15.

Schmitt, T. 2007. Molecular biogeography of Europe: Pleistocene cycles and postglacial trends. Frontiers in Zoology 4: 1–13.

Sissom, W.D. 1994. Systematic studies on the genus *Megacormus* (Scorpiones, Chactidae, Megacorminae), with descriptions of a new species from Oaxaca, Mexico and of the male of *Megacormus segmentatus* Pocock. Insecta Mundi 8: 265–271.

Sissom, W.D., G.A. Polis, and D.D. Watt. 1990. Field and laboratory methods. *In* G.A. Polis (editor), The biology of scorpions: 215–221. Stanford, CA: Stanford University Press.

Skilodimou, H.D., G.D. Bathrellos, H. Maroukian, and K. Gaki-Papanastassiou. 2014. Late Quaternary evolution of the lower reaches of Ziliana stream in south Mt. Olympus (Greece). Geografia Fisica e Dinaminca Quaternaria 37: 43–50.

Smith, G.W., R.D. Nance, and A.N. Genes. 1997. Quaternary glacial history of Mount Olympus, Greece. Geological Society of America Bulletin 109: 809–824.

Soleglad, M.E., and W.D. Sissom 2001. Phylogeny of the family Euscorpiidae: A major revision. *In* V. Fet and P.A. Selden (editors), Scorpions 2001: in memoriam Gary A. Polis: 25–111. Burnham Beeches, Bucks, U.K.: British Arachnological Society.

Stahnke, H. L. 1970. Scorpion nomenclature and mensuration. Entomological News 81: 297–316.

Stahnke, H.L. 1972. UV light, a useful field tool. BioScience 22: 604–607.

Stamou, G.P., S. Sgardelis, and N.S. Margaris. 1984. Arthropods distribution pattern on a mountain gradient (Mt. Olympus, Greece). Revue d'Ecologie et de Biologie du Sol 21: 491–505.

Stockwell, S.A. 1989. Revision of the phylogeny and higher classification of scorpions (Chelicerata). Ph.D. dissertation, University of California, Berkeley, 413 pp.

Strid, A. 1980. Wildflowers of Mount Olympus. Athens, Greece: Goulandris Natural History Museum, 362 pp.

Štundlová, J.J. Šmíd, P. Nguyen, and F. Šťáhlavskỳ. 2019. Cryptic diversity and dynamic chromosome evolution in Alpine scorpions (Euscorpiidae: *Euscorpius*). Molecular Phylogenetics and Evolution 134: 152–163.

Theodoropoulos, K., F. Xystrakis, E. Eleftheriadou, and D.A. Samaras. 2011. Vegetation zones and habitat types in the area of responsibility of the management agency of Olympus National Park. Scientific Annals of the Faculty of Forestry and Natural Environment ME/2002/45: 1–18. Thessaloniki: Aristotle University.

Thorell, T. 1876. On the classification of scorpions. Journal of Natural History 17: 1–15.

Tropea, G. 2013a. Reconsideration of the taxonomy of *Euscorpius tergestinus* (Scorpiones: Euscorpiidae). Euscorpius 162: 1–23.

Tropea, G. 2013b. A new species of *Euscorpius* Thorell, 1876 from the western Balkans (Scorpiones: Euscorpiidae). Euscorpius 174: 1–10.

Tropea, G. 2017. Reconsideration of some populations of *Euscorpius sicanus* complex in Italy (Scorpiones: Euscorpiidae). Arachnida – Rivista Aracnologica Italiana 11: 2–60.

Tropea, G., and R. Ozimec. 2020. Another new species of *Euscorpius* Thorell, 1876 from the caves of Croatia and Bosnia-Herzegovina (Scorpiones: Euscorpiidae), with notes on biogeography and cave ecology. Euscorpius 308: 1–13.

Tropea, G., V. Fet, A. Parmakelis, P. Kotsakiozi, and I. Stathi. 2014. Three new species of *Euscorpius* (Scorpiones: Euscorpiidae) from Greece. Euscorpius 190: 1–22.

Tropea, G., V. Fet, A. Parmakelis, and I. Stathi. 2022. Two new species of *Euscorpius* (Scorpiones, Euscorpiidae) from Skyros and Andros Islands, Greece. Zoodiversity 56: 307–322.

Ursenbacher, S., M. Carlsson, V. Helfer, H. Tegelström, and L. Fumagalli. 2006. Phylogeography and Pleistocene refugia of the adder (*Vipera berus*) as inferred from mitochondrial DNA sequence data. Molecular Ecology 15: 3425–3437.

Vachon, M. 1948. Scorpions récoltes dans l'île de Crête par Mr le Docteur Otto von Wettstein. Annalen des Naturhistorischen Museums in Wien 56: 61–69.

Vachon, M. 1952. Étude sur les scorpions. Algiers: Institut Pasteur d'Algérie, 482 pp.

Vachon, M. 1963. De l'utilité, en systématique, d'une nomenclature des dents des chélicères chez les scorpions. Bulletin du Muséum Natonal d'Histoire Naturelle, Paris 35: 161–166.

Vachon, M. 1981. Remarques sur la classification sous-spécifique des espèces appartenant au genre *Euscorpius* Thorell, 1876 (Scorpionida, Chactidae). Comptes-Rendus 6ème Colloque d'Arachnologie d'Expression Française (Colloque International Européen), 1981 (Modena-Pisa)/Atti della Società Toscana di Scienze Naturali Memorie (B) 88: 193–203.

All issues of *Novitates* and *Bulletin* are available on the web (https://digitallibrary.amnh.org/handle/2246/5). Order printed copies on the web from:
https://shop.amnh.org/books/scientific-publications.html

or via standard mail from:
American Museum of Natural History—Scientific Publications
Central Park West at 79th Street
New York, NY 10024

♾ This paper meets the requirements of ANSI/NISO Z39.48-1992 (permanence of paper).